Effect of the Dihedral Angle of Biaryl-Bridged Bisphosphite Ligands on Enantioselectivity and Regioselectivity of Asymmetric Hydroformylation

Christopher J. Cobley,† Robert D. J. Froese, Jerzy Klosin,* Cheng Qin, and Gregory T. Whiteker*,‡

Corporate R&D, The Dow Chemical Company, 1776 Building, Midland, Michigan 48674

Khalil A. Abboud

Department of Chemistry, University of Florida, Gainesville, Florida 32611

Received November 20, 2006

Eight new biaryl-bridged bisphosphite ligands have been synthesized and applied in rhodium-catalyzed asymmetric hydroformylation of styrene, allyl cyanide, and vinyl acetate. X-ray crystallographic studies of square planar LRh(acac) complexes of four of these bisphosphite ligands revealed that the dihedral angle of the bridging biaryl moiety depends on its identity and lies between 59.8° and 80.0°. A correlation between the dihedral angle in these Rh complexes and hydroformylation enantioselectivity and regioselectivity for both allyl cyanide and vinyl acetate is reported. Smaller dihedral angles were found to lead to increased regio- and enantioselectivity. Density functional theory calculations of a five-coordinate model complex ($LRh(CO)_2H$) show that decreased dihedral angles lead to smaller P−Rh−P bite angles. Although large bite angles have previously been correlated with increased hydroformylation regioselectivity, these results provide the first demonstration of a bite angle effect on enantioselectivity in asymmetric hydroformylation.

Introduction

Rhodium-catalyzed hydroformylation of α-olefins is widely used for the industrial synthesis of alcohols, carboxylic acids, and other aldehyde derivatives.[1] Phosphites are highly effective ligands for rhodium-catalyzed olefin hydroformylation[2] and can offer increased reaction rates[3] and chemoselectivity[4] over conventional phosphine ligands.[5] The modular structure of bisphosphite ligands based upon ubiquitous diols has made tailoring of regiocontrol possible. For example, Biphephos leads to high selectivity for the linear aldehyde regioisomer, which is typically desired for commodity chemical applications.[6] A related biphenol-based bisphosphite ligand, Chiraphite, was developed for branched-selective, asymmetric hydroformylation of vinyl arenes.[7,8]

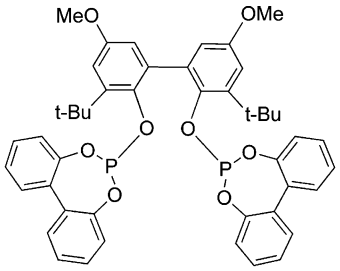

Biphephos

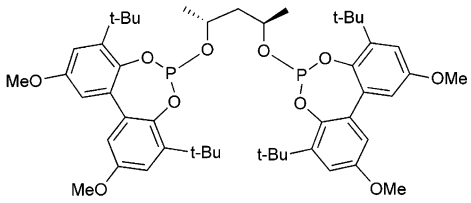

(*R*,*R*)-Chiraphite

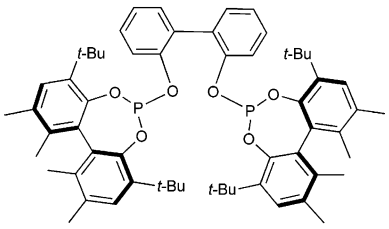

(*S*,*S*)-Kelliphite

We recently reported a new class of optically active bisphosphite ligands for use in asymmetric hydroformylation. Unlike

* Corresponding authors: E-mail: jklosin@dow.com; whitekgt2@dow.com.

† Dowpharma, Chirotech Technology Limited, a subsidiary of The Dow Chemical Company, 162 Cambridge Science Park, Cambridge CB4 0GH, UK.

‡ Current address: Dow Agrosciences, 9330 Zionsville Rd., Indianapolis, Indiana 46268.

(1) (a) *Rhodium Catalyzed Hydroformylation*; Claver, C., van Leeuwen, P. W. N. M., Eds.; Kluwer Academic Publishers: Dordrecht, 2000. (b) Bohnen H.; Cornils, B. *Adv. Catal.* **2002**, *47*, 1−64.

(2) Pruett, R. L.; Smith, J. A. *J. Org. Chem.* **1969**, *34*, 327−330.

(3) van Leeuwen, P. W. N. M.; Roobeek, C. F. *J. Organomet. Chem.* **1983**, *258*, 343−350.

(4) Cuny, G. D.; Buchwald, S. L. *J. Am. Chem. Soc.* **1993**, *115*, 2066−2068.

(5) For recent examples of active phosphine catalysts in asymmetric hydroformylation: (a) Clark, T. P.; Landis, C. R.; Freed, S. L.; Klosin, J.; Abboud, K. A. *J. Am. Chem. Soc.* **2005**, *127*, 5040−5042. (b) Axtell, A. T.; Cobley, C. J.; Klosin, J.; Whiteker, G. T.; Zanotti-Gerosa, A.; Abboud K. A. *Angew. Chem., Int. Ed.* **2005**, *44*, 5834−5838. (c) Axtell, A. T.; Klosin, J.; Abboud, K. A. *Organometallics* **2006**, *25*, 5003−5009.

(6) Billig, E.; Abatjoglou, A. G.; Bryant, D. R. US. Patents 4,668,651 (1987) and 4,769,498 (1988).

10.1021/om061065z CCC: $37.00
Publication on Web 05/02/2007

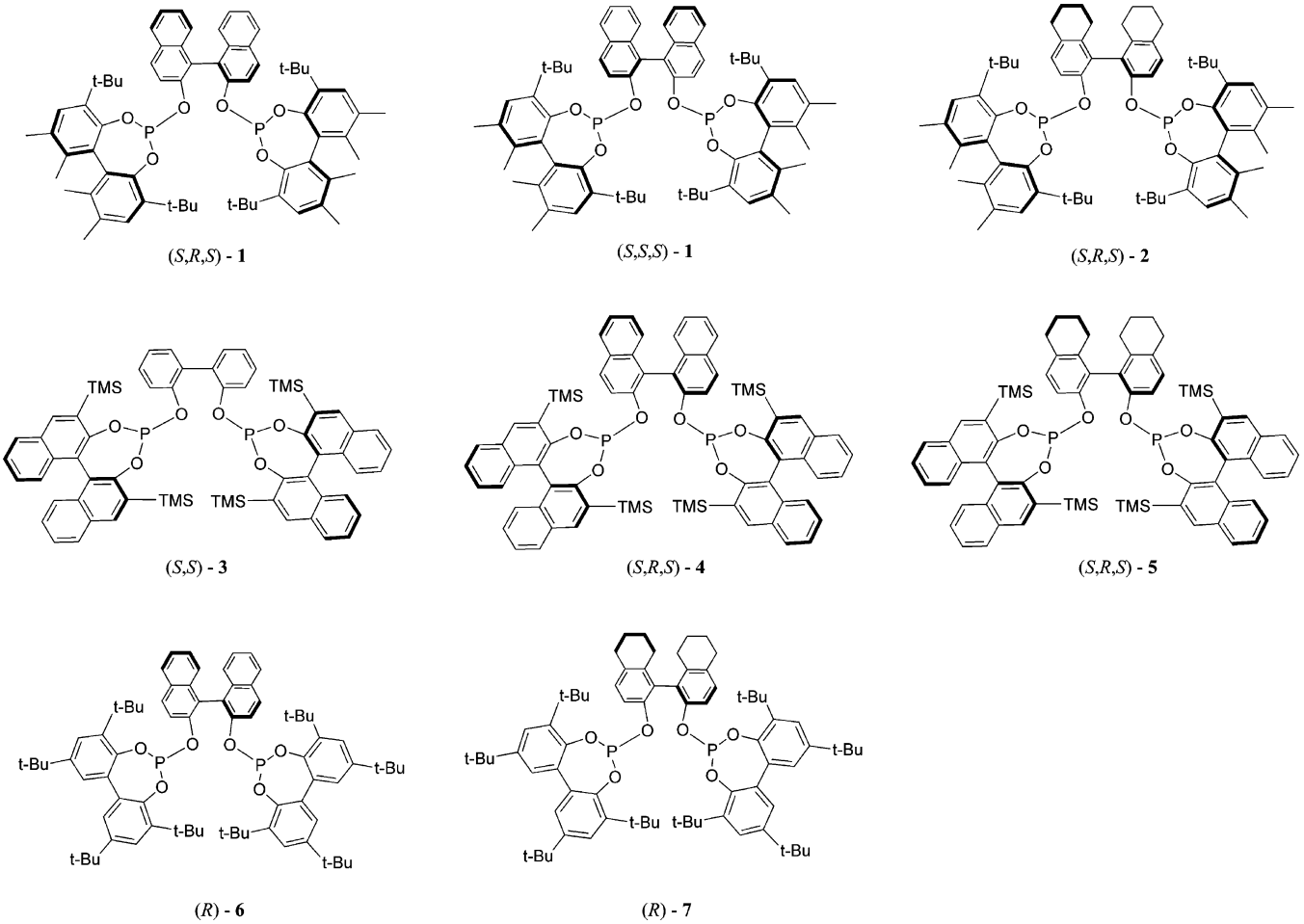

Figure 1. Ligands prepared and studied in asymmetric hydroformylation reactions.

Chiraphite, which contains epimerizable biaryl moieties, these ligands contain conformationally rigid, optically active dibenzo-[*d*,*f*][1,3,2]dioxaphosphepin moieties bridged by simple achiral diols.[9] The advantage of this ligand design is that simple changes in the achiral bridging diol can have significant effects on catalyst performance. We were mainly interested in the ability of this particular ligand design to control ligand bite angle, a structural feature that has been demonstrated to influence hydroformylation regioselectivity of terminal olefins.[10] Indeed, analogues of Chiraphite with different bridging diolate lengths were reported by van Leeuwen to exert significantly lower enantio- and regiocontrol.[8a] This new ligand class, however, is more synthetically accessible since it does not require optically active diols, but instead utilizes the commercially available (*S*)-3,3′-di-*tert*-butyl-5,5′,6,6′-tetramethylbiphenyl-2,2′-diol (BIPHEN-H_2)[11] as a chiral auxiliary. Of these new bisphosphite ligands, the 2,2′-biphenol-bridged ligand, (*S*,*S*)-Kelliphite, was found to exhibit particularly high regiochemical and stereochemical control for the asymmetric hydroformylation of both allyl cyanide[9] and vinyl acetate.[12] Chiraphite was found to offer poor selectivity with these substrates. In this paper we present our studies aimed at understanding the factors that influence hydroformylation regio- and enantioselectivity using biaryl-bridged ligands related to (*S*,*S*)-Kelliphite in asymmetric hydroformylation of styrene, allyl cyanide, and vinyl acetate. Reported herein are the syntheses of (*S*,*S*)-Kelliphite analogues where the bridging biaryl group has been systematically altered to vary its dihedral angle. Single-crystal X-ray analyses of five different rhodium complexes confirmed that changes in substituents in the 6,6′ position of the bridging biaryl groups influence its dihedral angle.

Results and Discussion

The new bisphosphite ligands prepared in this study are presented in Figure 1. (*S*,*S*)-Kelliphite can potentially adopt two diastereoisomeric structures, which are interconvertible by rotation about the central biaryl bond. Previous studies have demonstrated facile epimerization of all three biaryls in Biphephos.[13] van Leeuwen has observed chiral cooperativity in

(7) (a) Babin J. E.; Whiteker G. T. WO 93/03830, 1992. (b) Whiteker, G. T.; Briggs, J. R.; Babin, J. E.; Barner, B. A. In *Catalysis of Organic Reactions*; Marcel Dekker, Inc.: New York, 2003; Vol. 89, pp 359−367.

(8) (a) Buisman, G. J. H.; Vos, E. J.; Kamer, P. C. J.; van Leeuwen, P. W. N. M. *J. Chem. Soc., Dalton Trans.* **1995**, 409−417. (b) Buisman, G. J. H.; van der Veen, L. A.; Klootwijk, A.; de Lange, W. G. J.; Kamer, P. C. J.; van Leeuwen, P. W. N. M.; Vogt, D. *Organometallics* **1997**, *16*, 2929−2939.

(9) Cobley, C. J.; Gardner, K.; Klosin, J.; Praquin, C.; Hill, C.; Whiteker, G. T.; Zanotti-Gerosa, A.; Petersen, J. L.; Abboud, K. A. *J. Org. Chem.* **2004**, *69*, 4031−4040.

(10) For effects of catalyst bite angle on selectivity in hydroformylation reactions see: (a) Casey, C. P.; Whiteker, G. T.; Melville, M. G.; Petrovich, L. M.; Gavney, J. A., Jr.; Powell, D. R. *J. Am. Chem. Soc.* **1992**, *114*, 5535−5543. (b) Kamer, P. C. J.; van Leeuwen, P. W. N. M.; Reek, J. N. H. *Acc. Chem. Res.* **2001**, *34*, 895−904.

(11) Enantiomerically pure BIPHEN-H_2 is commercially available from Strem.

(12) Cobley, C. J.; Klosin, J.; Qin, C.; Whiteker, G. T. *Org. Lett.* **2004**, *6*, 3277−3280.

(13) Briggs, J.R.; Whiteker, G. T. *Chem. Commun.* **2001**, 2174−2175.

Scheme 1. General Method for Synthesis of Bisphosphite Ligands[a]

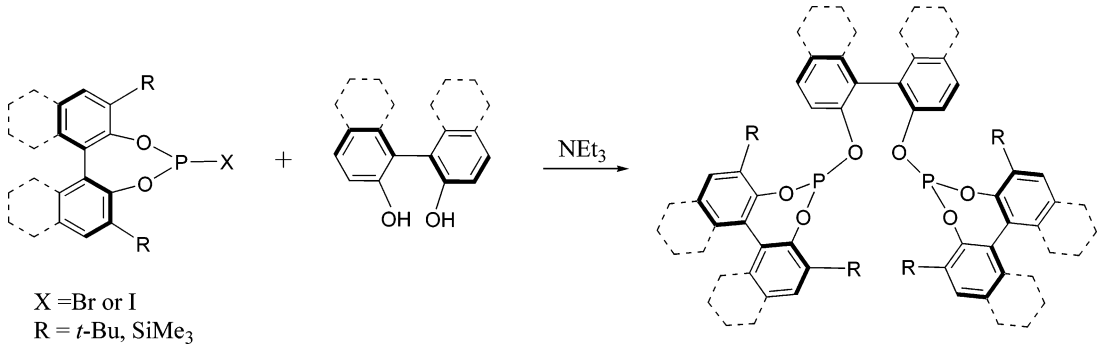

[a] Reactions were performed in the presence of NEt_3 (2.2 equiv/diol) at ambient temperature in toluene in an N_2-filled glovebox.

Chiraphite analogues and that nonepimerizable, conformationally stable bisphosphite diastereoisomers can significantly differ in their performance in asymmetric hydroformylation of vinyl arenes.[8b] Similar differences between conformationally stable bisphosphite diastereoisomers were also observed in achiral propylene hydroformylation with linear-selective ligands related to Biphephos.[13] Ligands (*S,R,S*)-**1** and (*S,R,S*)-**2** are analogues of (*S,S*)-Kelliphite that are bridged by configurationally stable, optically active biaryls. The absolute configuration of bisphosphites (*S,R,S*)-**1** and (*S,R,S*)-**2** is the same as that observed in the crystal structure of (*S,S*)-Kelliphite and [(*S,S*)-Kelliphite]-Rh(acac).[9] Ligand (*S,R,S*)-**1**, bridged by an (*R*)-binaphthyl moiety, and ligand (*S,R,S*)-**2**, bridged by (*R*)-octahydrobinaphthyl, should exhibit similar catalytic performance to (*S,S*)-Kelliphite if epimerization of the bridging biaryl in (*S,S*)-Kelliphite does not occur during catalysis. A diastereoisomer bridged by (*S*)-binaphthyl, (*S,S,S*)-**1**, was also prepared to evaluate the importance of the relative stereochemistry of the bridging biaryl and dioxaphosphepin fragment on catalytic performance.

Bisphosphite (*S,S*)-**3**, which utilizes (*S*)-3,3′-bis(trimethylsilyl)-1,1′-binaphthol in place of (*S*)-BIPHEN-H_2, was also synthesized to study the effect of replacement of *t*-Bu substituents by $SiMe_3$ substituents in ligands structurally related to (*S,S*)-Kelliphite. Two additional ligands based on (*S*)-3,3′-bis-(trimethylsilyl)-1,1′-binaphthol [(*S,R,S*)-**4** and (*S,R,S*)-**5**] were also prepared to evaluate the effect of the bridging biaryl moiety. Bisphosphites (*S,R,S*)-**4** and (*S,R,S*)-**5** are bridged by (*R*)-binaphthyl and (*R*)-octahydrobinaphthyl, respectively. These (*S*)-3,3′-bis(trimethylsilyl)-1,1′-binaphthol-based ligands provide an additional series for comparison to (*S*)-BIPHEN-based bisphosphites. The motivation for these syntheses came from the work of van Leeuwen et al., who reported that Chiraphite analogues prepared from 3,3′-$SiMe_3$-substituted biphenols lead to higher enantioselectivity.[8b]

In addition to these conformationally rigid analogues of (*S,S*)-Kelliphite, a structural design reminiscent of Chiraphite was employed in bisphosphites (*R*)-**6** and (*R*)-**7**, which reverses the position of the chiral auxiliary from the end groups to the ligand backbone. Ligands (*R*)-**6** and (*R*)-**7** contain an optically active bridging biaryl moiety in combination with a conformationally flexible dibenzo[*d*,f][1,3,2]dioxaphosphepin fragment.

Bisphosphite ligands were prepared by the reaction of optically active phosphorobromidite or phosphoroiodidite with the appropriate diol, as illustrated in Scheme 1. Bisphosphites were obtained as white powders after filtration of triethylammonium salt, evaporation of toluene from the filtrate, and trituration with MeCN. Products were characterized by ^1H, $^{13}C\{^1H\}$, and $^{31}P\{^1H\}$ NMR, HRMS, elemental analysis, and, in the case of (*S,S*)-**3**, X-ray single-crystal analysis.[14] The $^{31}P\{^1H\}$ NMR spectra show a singlet in the range δ 132−142 ppm consistent with C_2 symmetry. The $^{31}P\{^1H\}$ NMR resonances of ligands (*R*)-**6** and (*R*)-**7**, however, were broadened ($\Delta\nu_{1/2}$ = 29 and 13 Hz for **6** and **7**, respectively) and suggested fluxionality of the tetra-*tert*-butylbiphenyl fragments.

It is important to use anhydrous solvents during syntheses of these phosphite ligands, as the phosphorobromidite and phosphoroiodidite undergo facile hydrolysis by trace water, leading to formation of phosphinic acid derivatives. In our first attempt to synthesize **7**, traces of water in the solvent led to partial hydrolysis of the corresponding iodidite, as evidenced by a singlet at 11 ppm in the $^{31}P\{^1H\}$ NMR spectrum. When ligand **7**, contaminated with small amounts of this aryl phosphonate, was subsequently reacted with [(1,5-cyclooctadiene)Rh(acac)], the expected complex was formed together with small amounts of other species. After a few days at room temperature a few crystals appeared in the NMR tube. Single-crystal X-ray analysis of this material showed it to be a dimer,[14] which most likely formed as a result of reaction of the phosphonate derivative with [(1,5-cyclooctadiene)Rh(acac)] (eq 1).

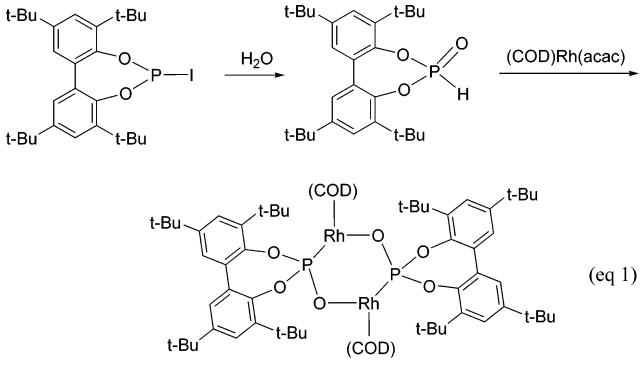

(eq 1)

Rh-dimer

Hydroformylation Study. Asymmetric hydroformylation experiments were performed in an Argonaut Endeavor reactor system consisting of eight parallel stirred autoclaves. Catalysts were generated *in situ* from the reaction of the appropriate ligand (1.2 equiv) with $Rh(CO)_2(acac)$ in toluene at 150 psi syn gas ($CO:H_2$ 1:1). Hydroformylation reactions were performed for 3 h with molar substrate to catalyst ratios of 500 at 35 °C and 1000 at 70 °C. Ligands were evaluated as previously described using an olefin mixture composed of styrene, allyl cyanide, and vinyl acetate in 1:1:1 molar ratio.[12] Chiral GC analyses allowed determination of conversion, regioselectivity (branched/linear),

(14) See Supporting Information for details.

Table 1. Asymmetric Hydroformylation of Styrene, Allyl Cyanide, and Vinyl Acetates, with Bisphosphite Ligands[a]

			styrene			allyl cyanide			vinyl acetate		
entry	L	*T* (°C)	conv[b]	b:l[c]	% ee	conv[b]	b:l[c]	% ee	conv[b]	b:l[c]	% ee
1	Kelliphite	35	48	71.3	16 (*S*)	99	15.0	76 (*S*)	24	112.1	87 (*R*)
		70	95	16.9	1 (*S*)	100	10.6	70 (*S*)	88	63.5	77 (*R*)
2	(*S*,*R*,*S*)-**1**	35	39	44.9	2 (*R*)	98	11.0	65 (*S*)	18	93.7	86 (*R*)
		70	90	10.9	24 (*R*)	100	8.5	59 (*S*)	85	48.1	74 (*R*)
3	(*S*,*S*,*S*)-**1**	35	40	12.1	15 (*R*)	59	3.3	23 (*R*)	9	24.5	7 (*S*)
		70	84	1.7	5 (*R*)	100	2.5	12 (*R*)	81	47.3	3 (*S*)
4	(*S*,*R*,*S*)-**2**	35	25	46.9	12 (*S*)	84	8.5	62 (*S*)	10	66.3	71 (*R*)
		70	84	12.9	13 (*R*)	100	7.0	58 (*S*)	71	37.5	60 (*R*)
5	(*S*,*S*)-**3**	35	7	24.5	43 (*S*)	36	19.3	63 (*S*)	2	58.5	73 (*R*)
		70	52	7.1	32 (*S*)	100	10.7	48 (*S*)	34	28.8	55 (*R*)
6	(*S*,*R*,*S*)-**4**	35	6	10.4	5 (*S*)	29	8.7	38 (*S*)	4	43.9	50 (*R*)
		70	37	3.9	9 (*S*)	99	5.3	22 (*S*)	37	25.1	43 (*R*)
7	(*S*,*R*,*S*)-**5**	35	6	7.3	1 (*R*)	42	6.5	24 (*S*)	4	31.8	17 (*S*)
		70	57	3.2	1 (*R*)	100	3.8	3 (*S*)	53	18.4	12 (*S*)
8	(*R*)-**6**	35	9	49.8	15 (*S*)	48	9.2	48 (*S*)	7	80.5	12 (*R*)
		70	50	15.1	15 (*R*)	100	7.5	45 (*S*)	66	59.5	10 (*R*)
9	(*R*)-**7**	35	5	57.2	7 (*R*)	37	18.6	15 (*S*)	9	126.1	56 (*S*)
		70	32	13.1	25 (*R*)	99	13.7	15 (*S*)	69	103.2	44 (*S*)

[a] Reaction conditions: 150 psi 1:1 H_2/CO, ligand:Rh = 1.2:1, solvent = acetone (35 °C runs) and toluene (70 °C runs), molar ratio of olefin:Rh = 500:1 at 35 °C and 1000:1 at 70 °C. [b]Percentage conversion of olefins after 3 h. [c]b/l = branched to linear ratio.

Table 2. Selected Bond Lengths (Å) and Angles (deg) for Rh(acac) Complexes of (*S*,*S*)-Kelliphite, (*S*,*R*,*S*)-1, (*S*,*R*,*S*)-2, (*S*,*R*,*S*)-4, and (*R*)-7

bond/angle	(*S*,*S*-Kelliphite)-Rh(acac)[17]	[(*S*,*R*,*S*)-**1**]-Rh(acac)	[(*S*,*R*,*S*)-**2**]-Rh(acac)	[(*S*,*R*,*S*)-**4**]-Rh(acac)	[(*R*)-**7**]Rh(acac)[17]
P1−O4	1.601(5), 1.614(5)	1.604(2)	1.605(2)	1.602(3)	1.597(3), 1.612(3)
P1−O5	1.610(4), 1.625(4)	1.630(2)	1.627(2)	1.643(3)	1.629(3), 1.611(3)
P1−O6	1.636(5), 1.622(5)	1.615(2)	1.615(2)	1.610(3)	1.592(3), 1.618(3)
P2−O1	1.608(5), 1.611(5)	1.604(2)	1.610(2)	1.643(3)	1.601(3), 1.607(2)
P2−O2	1.631(4), 1.611(5)	1.630(2)	1.630(2)	1.630(3)	1.620(3), 1.603(3)
P2−O3	1.619(4), 1.615(5)	1.608(2)	1.602(2)	1.615(4)	1.601(2), 1.622(3)
O4−P1−O5	100.3(2), 100.4(2)	98.07(9)	98.11(11)	99.2(2)	98.2(1), 99.8(1)
O4−P1−O6	96.5(2), 98.0(2)	99.43(9)	100.02(11)	98.4(2)	100.0(1), 103.4(1)
O5−P1−O6	103.2(2), 103.2(2)	104.05(9)	103.09(11)	99.2(2)	104.2(1), 103.4(1)
O1−P2−O2	98.1(2), 97.1(2)	97.70(8)	96.9(1)	99.8(2)	97.1(1), 101.0(1)
O2−P2−O3	99.9(2), 101.2(3)	103.05(9)	103.93(11)	102.1(2)	103.3(1), 102.5(1)
O1−P2−O3	103.0(2), 102.2(2)	99.18(8)	100.44(12)	98.6(2)	100.6(1), 96.7(1)
Rh−O7	2.077(5), 2.084(5)	2.055(2)	2.069(2)	2.055(3)	2.052(3), 2.070(3)
Rh−O8	2.085(5), 2.053(4)	2.062(2)	2.056(2)	2.047(4)	2.080(3), 2.072(3)
P1−P2	3.234, 3.234	3.266	3.322	3.322	3.316, 3.304
Rh−P1	2.149(2), 2.140(2)	2.1436(7)	2.1563(8)	2.149(2)	2.150(1), 2.144 (1)
Rh−P2	2.145(2), 2.147(2)	2.1489(7)	2.1576(9)	2.150(2)	2.149(1), 2.146(1)
P2−Rh−P1 (bite angle)	97.74(8), 97.94(7)	99.06(3)	100.71(3)	101.20(5)	101.14(5), 100.70(4)
P1−Rh−O7	88.6(2), 85.5(2)	84.92(5)	85.86(7)	87.0(1)	83.28(8), 85.32(9)
P2−Rh−O8	85.0(2), 87.2(2)	87.86(5)	84.05(7)	82.9(1)	85.87(8), 83.77(8)
O7−Rh−O8	88.9(2), 88.9(2)	89.05(7)	89.32(9)	89.7(2)	90.0(1), 90.4(1)
$\theta_{A/B}$ (dihedral angle)	63.1, 62.3	67.6	62.9	61.0	46.7, 43.6
$\theta_{C/D}$ (dihedral angle)	60.5, 59.8	69.3	77.1	71.0	78.8, 80.0
$\theta_{E/F}$ (dihedral angle)	63.8, 58.4	60.4	57.7	62.7	43.9, 46.5

and enantioselectivity of all products derived from hydroformylation of all three olefins. Hydroformylation results are given in Table 1. Notably, none of the ligands in this study led to synthetically useful levels of enantioselectivity for styrene hydroformylation.

Bisphosphite (*S*,*R*,*S*)-**1** exhibited high regio- and enantiocontrol similar to that observed with (*S*,*S*)-Kelliphite using both allyl cyanide and vinyl acetate substrates. The (*S*,*S*,*S*)-**1** diastereoisomer, however, led to much lower selectivities than its *S*,*R*,*S* diastereoisomer. For this reason subsequent syntheses of bisphosphite ligands focused only on (*S*,*R*,*S*) diastereoisomers. Bisphosphite (*S*,*S*,*S*)-**1** also led to a reversal of the absolute configuration of allyl cyanide and vinyl acetate hydroformylation products. For example, asymmetric hydroformylation of vinyl acetate at 35 °C using (*S*,*R*,*S*)-**1** led to product with 86% ee (*S*) whereas (*S*,*S*,*S*)-**1** resulted in only 7% ee (*R*). In addition, the regioselectivity for branched aldehydes derived from all three olefins was much lower for (*S*,*S*,*S*)-**1** than for both (*S*,*S*)-Kelliphite and (*S*,*R*,*S*)-**1**. A related ligand that employs a bridging octahydrobinaphthol moiety, (*S*,*R*,*S*)-**2**, also exhibited comparable regioselectivities and enantioselectivities to both (*S*,*S*)-Kelliphite and (*S*,*R*,*S*)-**1**. Previously, we reported the X-ray structure of [(*S*,*S*)-Kelliphite]Rh(acac), which was shown to adopt the *S*,*R*,*S* configuration in the solid state.[9] These combined structural and hydroformylation results strongly suggest that the central epimerizable biaryl moiety in (*S*,*S*)-Kelliphite preferentially adopts the *R* configuration during catalysis. Similar chiral cooperativity in rhodium-catalyzed styrene hydroformylation was previously observed with biaryl-based bisphosphite ligands related to Chiraphite.[8b] It was shown that diastereoisomeric bisphosphites exhibited very different regio- and enantioselectivities in styrene hydroformylation.[8b] This study concluded that Chiraphite−Rh complex preferentially adopts one diastereoisomeric configuration. Analogous effects have been observed on the regioselectivity of the achiral hydroformylation of propylene.[13]

Bisphosphite (*S*,*S*)-**3** gave hydroformylation results comparable to those of (*S*,*S*)-Kelliphite. The same configuration of

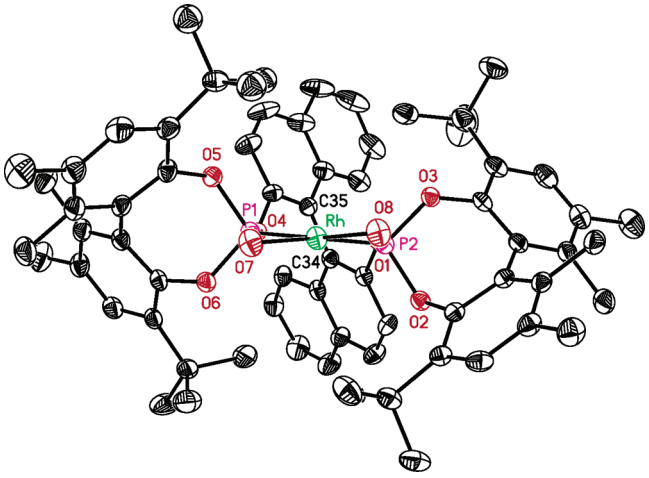

Figure 2. Molecular structure and labeling scheme for [(*S*,*R*,*S*)-**1**]Rh(acac) with 40% probability thermal ellipsoids. Carbon atoms of the acac fragment and all hydrogen atoms were removed for clarity.

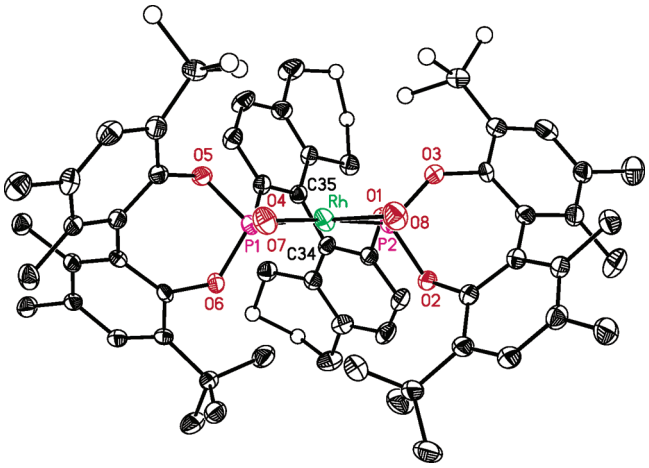

Figure 3. Molecular structure and labeling scheme for [(*S*,*R*,*S*)-**2**]Rh(acac) with 40% probability thermal ellipsoids. Carbon atoms of the acac fragment and all hydrogen atoms were removed for clarity.

aldehyde products was obtained using (*S*,*S*)-Kelliphite and (*S*,*S*)-**3**. Hydroformylation of styrene using (*S*,*S*)-**3** proceeded with higher enantioselectivity (43% ee vs 16% ee) but significantly lower regioselectivity (b/l = 24.5 vs 71.3) than with (*S*,*S*)-Kelliphite. The selectivities obtained with allyl cyanide and vinyl acetate were somewhat lower with bisphosphite (*S*,*S*)-**3** than (*S*,*S*)-Kelliphite.

Bisphosphite (*S*,*R*,*S*)-**4**, which contains a bridging (*R*)-binaphthol moiety, exhibited significantly reduced levels of regio- and enantiocontrol when compared to the configurationally flexible bisphosphite (*S*,*S*)-**3**. A further reduction in selectivity was observed with the octahydrobinaphthol-bridged bisphosphite (*S*,*R*,*S*)-**5**. In particular, for hydroformylation of vinyl acetate, bisphosphites (*S*,*R*,*S*)-**4** and (*S*,*R*,*S*)-**5** both exhibited lower levels of enantiocontrol (50% ee (*R*) and 17% ee (*S*), respectively) than (*S*,*S*)-**3**, which is bridged by an epimerizable biphenyl (73% ee (*R*)). In addition to these differences in enantioselectivity, the regioselectivity for branched aldehyde with all three substrates also decreased in the order (*S*,*S*)-**3** > (*S*,*R*,*S*)-**4** > (*S*,*R*,*S*)-**5**. These results suggest that (*S*,*S*)-**3** adopts an *SRS* configuration during catalysis analogously to that found in (*S*,*S*)-Kelliphite.

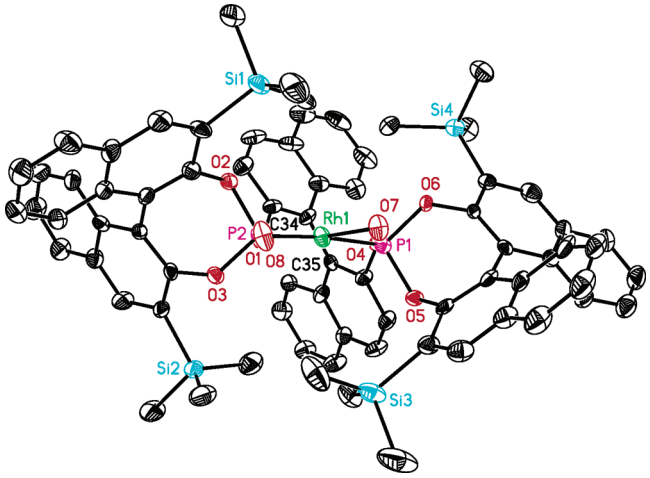

Figure 4. Molecular structure and labeling scheme for [(*S*,*R*,*S*)-**4**]Rh(acac) with 40% probability thermal ellipsoids. Carbon atoms of the acac fragment and all hydrogen atoms were removed for clarity.

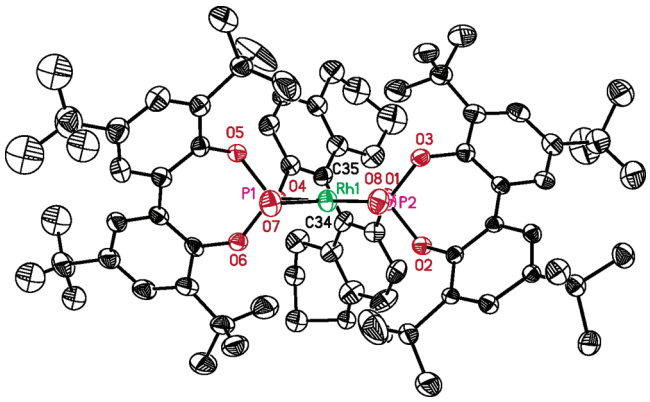

Figure 5. Molecular structure and labeling scheme for [(*R*)-**7**]Rh(acac) with 40% probability thermal ellipsoids. Carbon atoms of the acac fragment and all hydrogen atoms were removed for clarity.

Bisphosphites (*R*)-**6** and (*R*)-**7** employ an optically active bridging biphenol along with stereochemically nonrigid dibenzo[*d*,*f*][1,3,2]dioxaphosphepin moieties. The expectation was that the ligands' bridging chiral unit would direct the chirality of dibenzo[*d*,*f*][1,3,2]dioxaphosphepin fragments, thus imparting a similar chiral environment to that observed in (*S*,*S*)-Kelliphite. Surprisingly, the enantioselectivities produced by these two ligands are much lower than those observed with (*S*,*S*)-Kelliphite. For example, for allyl cyanide hydroformylation at 35 °C, bisphosphites (*R*)-**6** and (*R*)-**7** led to only 48% ee and 15% ee, respectively, whereas (*S*,*S*)-Kelliphite gave 76% ee under these conditions. It is notable that these ligands, which are bridged by a biaryl with *R* absolute configuration, led to the same product enantiomer (*S*) from allyl cyanide as that observed with (*S*,*S*)-Kelliphite. For vinyl acetate, however, the product enantioselectivity was dramatically reduced for (*R*)-**6** (12% ee, *R*) as compared to (*S*,*S*)-Kelliphite (87% ee, *R*). Interestingly, (*R*)-**7** led to higher enantioselectivity than (*R*)-**6** but shows reversal of product absolute configuration (56% ee, *S*). This effect of the bridging biaryl fragment is similar to that observed with binaphtyl-bridged (*S*,*R*,*S*)-**4** and octahydrobinaphthyl-bridged (*S*,*R*,*S*)-**5**. The differences between (*R*)-**6** and (*R*)-**7**, which contain epimerizable dibenzo[*d*,*f*][1,3,2]-dioxaphosphepin moieties, are, however, more pronounced.

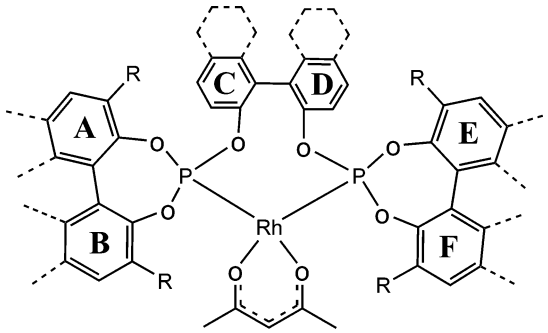

Figure 6. Representation of bisphosphite dihedral angles.

Despite these differences in enantioselectivities, the regioselectivities induced by (*S*,*S*)-Kelliphite, (*R*)-**6**, and (*R*)-**7** are comparable.

Synthesis and Structural Analysis of [(Bisphosphite)Rh(acac)] Complexes. To investigate conformational details of these newly prepared ligands upon coordination to the rhodium center, the synthesis of representative Rh complexes was undertaken. Bisphosphites (*S*,*R*,*S*)-**1**, (*S*,*R*,*S*)-**2**, (*S*,*R*,*S*)-**4**, (*R*)-**6**, and (*R*)-**7** were reacted with 1 equiv of [(1,5-cyclooctadiene)-Rh(acac)] in toluene solution, resulting in clean formation of [Bisphosphite]Rh(acac) complexes. All rhodium complexes were characterized by multinuclear and multidimensional NMR spectroscopy, HRMS, and in the case of [(*S*,*R*,*S*)-**1**]Rh(acac), [(*S*,*R*,*S*)-**2**]Rh(acac), [(*S*,*R*,*S*)-**4**]Rh(acac), and [(*R*)-**7**]Rh(acac) single-crystal X-ray analysis. All complexes exhibited C_2 symmetry in solution on the basis of NMR spectroscopy. The $^{31}P\{^1H\}$ NMR spectra show a doublet in the range δ 133−142 ppm (d, $^1J_{Rh-P}$ = 313−318 Hz).

Molecular structures of Rh(acac) complexes containing (*S*,*R*,*S*)-**1**, (*S*,*R*,*S*)-**2**, (*S*,*R*,*S*)-**4**, and (*R*)-**7** ligands were determined by single-crystal X-ray analysis. Selected bond and angle data for the structures are presented in Table 2 along with related data for [(*S*,*S*)-Kelliphite]Rh(acac).[9] A comprehensive listing of X-ray data is included in the Supporting Information. Thermal ellipsoid drawings for (*S*,*R*,*S*)-**1**, (*S*,*R*,*S*)-**2**, (*S*,*R*,*S*)-**4**, and (*R*)-**7** are shown in Figures 2, 3, 4, and 5, respectively. The geometry around the rhodium atom is close to idealized square planar in all of the complexes. In the solid state, all complexes have molecular C_2 symmetry with the Rh atom and the center of the bridging biaryl bond (C34−C35) lying on the 2-fold axis. The P1−Rh−P2 bite angles span a narrow range in these complexes [(*S*,*R*,*S*)-**1** (99.1°), (*S*,*R*,*S*)-**2** (100.7°), (*S*,*R*,*S*)-**4** (101.2°), and (*R*)-**7** (100.7/101.1°)] and fall within the range (93−105°) observed in other Rh(acac) complexes containing both monodentate[15] and bidentate phosphite ligands.[16] There are substantial differences between the dihedral angles ($\theta_{C/D}$) in complexes containing biphenyl (60.5°, 59.8° in (*S*,*S*)-Kelliphite), binaphthyl (69.3°, 71.0° in (*S*,*R*,*S*)-**1** and (*S*,*R*,*S*)-**4**), and octahydrobinaphthyl (77.1°, 78.8°, 80.0° in (*S*,*R*,*S*)-**2** and (*R*)-**7**) bridging groups (Table 2, Figure 6). The dihedral angles of the dibenzo[*d*,*f*]-[1,3,2]dioxaphosphepin units ($\theta_{A/B}$ and $\theta_{E/F}$) are significantly larger (within 57.7−67.6° range) in [(*S*,*R*,*S*)-**1**]Rh(acac), [(*S*,*R*,*S*)-**2**]Rh(acac), and [(*S*,*R*,*S*)-**4**]Rh(acac) than in the tetra-*tert*-butylphosphepin units of [(**7**)Rh(acac)] (Table 2). The increased dihedral angles ($\theta_{A/B}$ and $\theta_{E/F}$) in [(*S*,*R*,*S*)-**1**]Rh(acac), [(*S*,*R*,*S*)-**2**]Rh(acac), and [(*S*,*R*,*S*)-**4**]Rh(acac) complexes are due to the presence of the 6,6′-methyl substituents in the BIPHEN moiety. It is worth pointing out that the dihedral angles ($\theta_{C/D}$) of the octahydrobinaphthyl bridging unit in [(*S*,*R*,*S*)-**2**]Rh(acac) and [(**7**)Rh(acac)] are virtually the same despite substantial differences in $\theta_{A/B}$ and $\theta_{E/F}$ dihedral angles between phosphepin units in both of these complexes. This suggests that the identity of bridging units rather than their environment dictates the appropriate dihedral angle between aryl groups.

A close inspection of the structural and catalytic results suggests that the dihedral angle ($\theta_{C/D}$) of the bridging biphenol in these bisphosphite ligands may play a role in controlling hydroformylation selectivity. Figure 7 shows the relationship between $\theta_{C/D}$ in [(Bisphosphite)Rh(acac)] complexes and the enantioselectivity for asymmetric hydroformylation of both allyl cyanide and vinyl acetate. Complexes of bisphosphites **3** and **5** were not characterized crystallographically, so the dihedral angles for these ligands were approximated[18] to be the same as found for [(*S*,*S*)-Kelliphite)]Rh(acac) and [(*S*,*R*,*S*-**2**)Rh(acac)], respectively. As shown in Figure 7, the BIPHEN-based ligands (*S*,*S*)-Kelliphite, (*S*,*R*,*S*)-**1**, and (*S*,*R*,*S*)-**2** exhibit a linear relationship between $\theta_{C/D}$ and enantioselectivity with both allyl cyanide and vinyl acetate. No such correlation was evident with styrene, perhaps due to the low levels of enantioselectivity observed with these ligands for this olefinic substrate. A similar relationship between enantioselectivity and dihedral angle ($\theta_{C/D}$) for the 3,3′-bis(trimethylsilyl)-1,1′-bi-2,2′-naphthol-based bisphosphites, **3**−**5**, was also observed. The effect of decreased dihedral angle appears to be more pronounced in the 3,3′-bis-(trimethylsilyl)-1,1′-bi-2,2′-naphthol series of bisphosphite ligands.

Figure 8 shows the relationship between bridging dihedral angle ($\theta_{C/D}$) and regioselectivity for the branched aldehyde. For both allyl cyanide and vinyl acetate, increasing branched regioselectivity is correlated with a decrease in $\theta_{C/D}$. The regioselectivity for hydroformylation of allyl cyanide was found to be especially sensitive to changes in dihedral angle. BIPHEN-based and 3,3′-bis(trimethylsilyl)-1,1′-bi-2,2′-naphthol-based catalysts exhibited similar trends. No correlation between dihedral angle and regioselectivity was observed for styrene hydroformylation.

The lower enantioselectivities observed with bisphosphites (*R*)-**6** and (*R*)-**7** indicate that the mechanism of asymmetric induction in these bisphosphite ligands is not solely controlled by the dihedral angle of the bridging unit. Crystallographic data presented in Table 2 indicate that the dihedral angle ($\theta_{C/D}$) in [(*R*-**7**)Rh(acac)] is only slightly larger (av $\theta_{C/D}$ = 79.4°) than that in [(*S*,*R*,*S*-**2**)Rh(acac)] (77.1°), which is based on the

(15) (a) Leipoldt, J. G.; Lamprecht, G. J.; Van Zyl, G. J. *Inorg. Chem. Acta* **1985**, *96*, L31−L34. (b) Trzeciak, A. M.; Glowiak, T.; Grzybek, R.; Ziolkowski, J. J. *J. Chem. Soc., Dalton Trans.* **1997**, 1831−1837. (c) Esteruelas, M. A.; Lahoz, F. J.; Onate, E.; Oro, L. A.; Rodríguez, L; Steinert, P.; Werner, H. *Organometallics* **1996**, *15*, 3436−3444. (d) Meetsma, A.; Jongsma, T.; Challa, G; van Leeuwen, P. W. N. M. *Acta Crystallogr., Sect. C: Cryst. Struct. Commun.* **1993**, *49*, 1160−1163.

(16) (a) Shum, S. P.; Pastor, S. D.; Rihs, G. *Inorg. Chem.* **2002**, *41*, 127−131. (b) Van den Beuken, E. K.; de Lange, W. G. J.; van Leeuwen, P. W. N. M.; Veldman, N.; Spek, A. L.; Feringa, B. L. *J. Chem. Soc., Dalton Trans.* **1996**, 3561−3569. (c) Jiang, Y.; Xue, S.; Yu, K.; Li, Z.; Deng, J.; Mi A.; Chan, A. S. C. *J. Organomet. Chem.* **1999**, *586*, 159−165. (d) Agbossou, F.; Carpentier, J.-F.; Hatat, C.; Kokel, N.; Mortreux, A.; Betz, P.; Goddard, R.; Kruger, C. *Organometallics* **1995**, *14*, 2480−2489. (c) Van Rooy, A.; Kamer, P. C. J.; Van Leeuwen, P. W. N. M.; Goubitz, K.; Fraanje, J.; Veldman, N.; Spek, A. L. *Organometallics* **1996**, *15*, 835−847.

(17) Since there are two independent molecules in the asymmetric unit, two values for each bond distance and angle are provided.

(18) This approximation should be valid as dihedral angles $\theta_{C/D}$ of the binaphthyl fragments in [(*S*,*R*,*S*)-**4**]Rh(acac) and [(*S*,*R*,*S*)-**1**]Rh(acac) and the octahydrobinaphthyl bridging units in [(*S*,*R*,*S*)-**2**]Rh(acac) and [(*R*)-**7**]-Rh(acac) are within 2°. Despite substantial differences in phosphepin units in [(*S*,*R*,*S*)-**2**]Rh(acac) and [(*R*)-**7**]Rh(acac), the dihedral angle of the octahydrobinaphthyl unit has not changed much. This suggests that the nature of the 6,6′-substituents of the biaryl bridging unit, rather than the nature of phosphepin fragments, dictates the size of the dihedral angle.

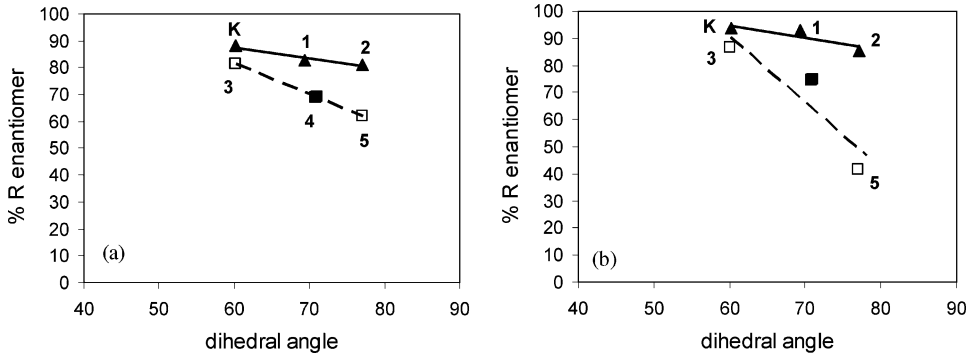

Figure 7. Effect of bridging biaryl dihedral angle, $\theta_{C/D}$, in [(Bisphosphite)Rh(acac)] complexes on enantioselectivity of asymmetric hydroformylation of (a) allyl cyanide and (b) vinyl acetate at 35 °C. Dihedral angles for (*S*,*S*)-Kelliphite] (K), **1**, **2**, and **4** were obtained from crystal structures of the corresponding [(Bisphosphite)Rh(acac)] complexes. Dihedral angles for ligands **3** and **5** (open squares) were approximated[18] to be the same as in (*S*,*S*)-Kelliphite and **2**, respectively.

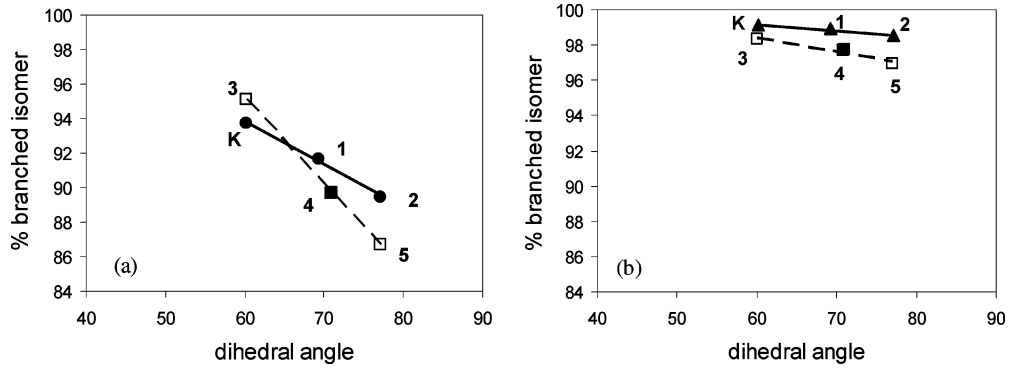

Figure 8. Effect of bridging biaryl dihedral angle, $\theta_{C/D}$, in [(Bisphosphite)Rh(acac)] complexes on regioselectivity of asymmetric hydroformylation of (a) allyl cyanide and (b) vinyl acetate at 35 °C. Dihedral angles for ligands **3** and **5** (open squares) were approximated[18] to be the same as in (*S*,*S*)-Kelliphite and **2**, respectively.

Table 3. Variation of the Bridging Biaryl Dihedral Angle, $\theta_{C/D}$, and Its Effect on the Bite Angle and Relative Energy (kcal/mol) for the Model Rhodium Catalyst, [(*S*,*S*)-Kelliphite]RhH(CO)$_2$

entry	$\theta_{C/D}$	P−Rh−P	ΔE
1	49.4	102.1	4.4
2	51.8	102.6	3.3
3	55.8	103.6	2.7
4	60.7	105.6	2.5
5	63.9	105.9	1.9
6	68.4	108.4	1.6
7	72.3	109.7	1.3
8	76.1	110.9	0.6
9	80.1	112.1	0.3
10	84.3	113.3	0.1
11	88.3	114.4	0.0
12	92.3	115.8	0.0
13	96.5	117.2	0.0
14	100.5	118.4	0.2
15	103.9	119.5	0.2
16	107.1	120.4	0.4
17	110.2	121.1	0.8

nonepimerizable BIPHEN. The enantioselectivities for asymmetric hydroformylation of allyl cyanide (15% ee) and vinyl acetate (56% ee) are much lower with *R*-**7** than would be expected solely on the basis of this small increase in $\theta_{C/D}$. The dihedral angles of the dibenzo[*d*,*f*][1,3,2]dioxaphosphepin units ($\theta_{A/B}$ and $\theta_{E/F}$) in [(*S*,*R*,*S*-**2**)Rh(acac)] are significantly larger than in the tetra-*tert*-butylphosphepin units of [(**7**)Rh(acac)]. The interplay of all three dihedral angles ($\theta_{A/B}$, $\theta_{C/D}$, and $\theta_{E/F}$) appears to be an important factor in achieving optimum asymmetric induction in this class of ligands.

To develop a better understanding of dihedral angle effects in biphenyl-bridged bisphosphite ligands on structural changes in corresponding Rh complexes, a computational study was undertaken. It was anticipated that these calculations could possibly provide insight into complex structural features that lead to increased hydroformylation selectivity as a result of decreased bridging biaryl dihedral angle. Of particular interest was the possibility that changes in this dihedral angle might be associated with changes in bite angle (P−Rh−P) of catalytic intermediates.[19,20] The influence of bite angle on regioselectivity of hydroformylation of terminal alkenes with rhodium−diphosphine catalysts has been well-established.[10,13] Although the X-ray structures of [(Bisphosphite)Rh(acac)] complexes described herein suggest a correlation between bridging dihedral angle and hydroformylation enantioselectivity, these four-coordinate complexes have an inherent electronic preference for a P−Rh−P bite angle of around 90°.[15,16] We therefore sought to study the effect of bridging dihedral angles in stereochemically flexible, five-coordinate Rh complexes, which are more relevant to the catalytic cycle. Spectroscopic studies using related bisphosphite ligands have revealed that the resting state under typical hydroformylation conditions is the five-coordinate (Bisphosphite)RhH(CO)$_2$ complex, which was used as the model for these computational studies.[21]

A series of density functional (DFT) calculations was performed in which the bridging biphenol dihedral angle was

(19) (a) Zhang, Z.; Qian, H.; Longmire, J.; Zhang, X. *J. Org. Chem.* **2000**, *65*, 6223. (b) Wu, S.; Wang, W.; Tang, W.; Lin, M.; Zhang, X. *Org. Lett.* **2002**, *4*, 4495−4497.

(20) (a) Saito, T.; Yokozawa, T.; Ishizaki, T.; Moroi, T.; Sayo, N.; Mirura, T.; Kumobayashi, H. *Adv. Synth. Catal.* **2001**, *343*, 264−267. (b) Jeulin, S.; de Paule, S. D.; Ratovelomanana-Vidal, V.; Genêt, J. P.; Champion, N.; Dellis, P. *Proc. Natl. Acad. Sci.* **2004**, *101*, 5799−5804.

(21) Moasser, B.; Gladfelter, W. L.; Roe, D. C. *Organometallics* **1995**, *14*, 3832−3838.

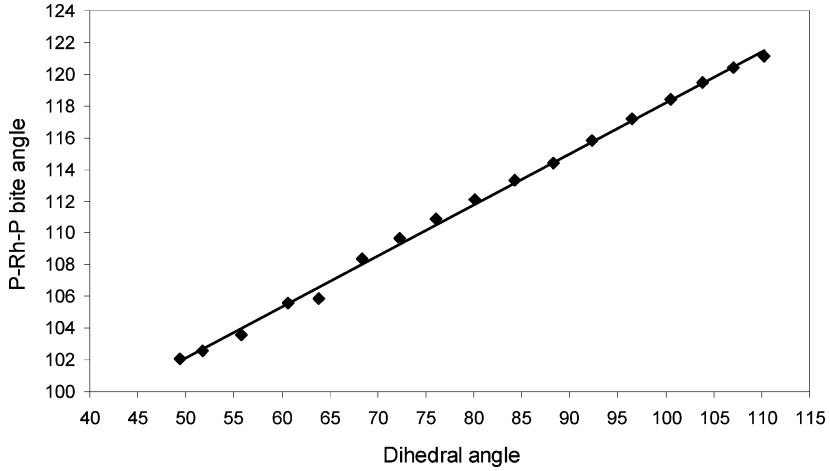

Figure 9. Relationship between dihedral angle of the bridging biaryl and P−Rh−P bite angle in the [(*S*,*S*)-Kelliphite]Rh(CO)$_2$H] complex based on DFT calculations.

systematically varied. For this purpose the (*S*,*S*)-Kelliphite ligand was utilized and the starting geometry of [(*S*,*S*)-Kelliphite]RhH-(CO)$_2$ was arranged to trigonal bipyramidal with two phosphorus atoms in the equatorial plane and an axial hydride. Seventeen structures were calculated[22] with torsion angle $\theta_{C/D}$ fixed[23] to values between 44° and 124°, while the remainder of the molecule was allowed to fully optimize.

Table 3 contains dihedral angle, $\theta_{C/D}$, the P−Rh−P bite angle, and the relative energy for all calculated structures. Despite a ±20° change in $\theta_{C/D}$ from fully relaxed structures (Table 3, entries 11−13), these structures resided only ca. 1 kcal/mol higher on the potential energy surface. The relatively small energy difference between calculated structures indicates the relative flexibility of the bridging biaryl in rhodium complexes of bisphosphites of this type. Increases in dihedral angle of the bridging biaryl are calculated by DFT to be accompanied by an increased P−Rh−P bite angle. As the dihedral angle of the bridge was increased from 49.4° to 110.2°, the bite angle increased linearly from 102.1° to 121.1° (Figure 9). The structures with dihedral angles in the range between 60° and 80° (range observed in synthesized complexes) are calculated to be within 2.2 kcal/mol in energy. The increased enantioselectivity and regioselectivity observed with bisphosphites that have smaller bridging dihedral angles ((*S*,*S*)-Kelliphite, **1**, and **3**) might therefore be a result of a decreased P−Rh−P bite angle. Although bite angle effects have been observed in linear-selective, achiral hydroformylation of terminal alkenes,[10] no reports of systematic bite angle effects in branched-selective, asymmetric hydroformylation have appeared.

Recently a number of reports of the effect of changes in dihedral angle in biaryl-bridged diphosphine ligands for asymmetric hydrogenation have appeared. The biaryl diphosphine ligands Segphos and Synphos gave higher enantioselectivities for asymmetric hydrogenation than observed with Binap.[20] The presence of smaller 6,6′-oxygen substituents in these ligands presumably allows smaller dihedral angles to be adopted than the binaphthalene-based BINAP ligand. The dihedral angle of the chiral biaryl bridge, calculated by molecular mechanics, was

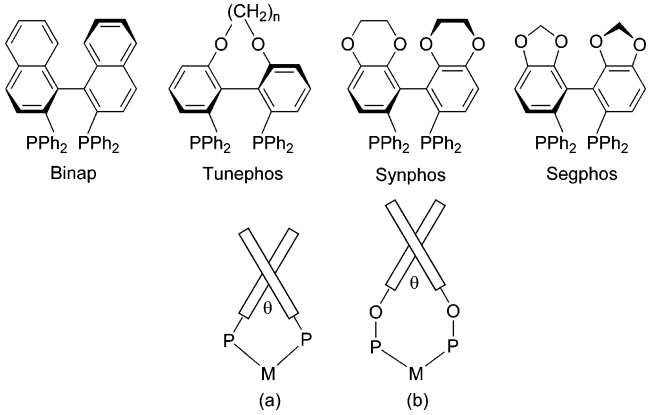

Figure 10. Schematic representation of biaryl chelate core. Binap, Synphos, Segphos, and Tunephos ligands are represented by structure a, whereas Kelliphite-type bisphosphites are represented by structure b.

stated to be correlated with the bite angle of the catalyst, and was proposed to influence the steric properties of these ligands. Systematic studies of the Tunephos family of bridged biaryl diphosphines by Zhang *et al*. have uncovered similar dihedral angle effects in enantioselective hydrogenation of both enol acetates and ketones.[19] On the basis of Cache MM2 molecular mechanics calculations, it was proposed that changes in the dihedral angle serve to tune the bite angle in the diphosphine−Rh catalysts. Optimum bridge lengths were found to be substrate-dependent and reflect the sensitivity of different reactions to bite angle. In Segphos, Synphos, and Tunephos, geometrical constraints force a decreased P−M−P bite angle when the bridging dihedral angle is decreased. This is due to the conformational rigidity imposed by the direct connection of the phosphorus atoms to the biaryl. Bisphosphites, such as (*S*,*S*)-Kelliphite, however, have greater conformational flexibility due to the intervening oxygen atoms (Figure 10). Our DFT calculations suggest that for the bisphosphite ligands reported in this study, decreases in bridging dihedral angle ($\theta_{C/D}$) are also accompanied by a decreased P−Rh−P bite angle. This decreased bisphosphite bite angle is proposed to be responsible for the increased enantioselectivity and branched regioselectivity observed with (*S*,*S*)-Kelliphite. These data are consistent with previous hydroformylation studies that showed that catalysts with a larger P−Rh−P bite angle lead to increased formation of linear isomer.[10]

(22) XYZ coordinates for all calculated structures are included in the Supporting Information. Additionally, a file in sd format containing all calculated structures is also included in the supporting materials. This file can be read by many programs including freely available Mercury (http://www.ccdc.cam.ac.uk/mercury/).

(23) While the torsion angle between two aryl rings of the bridging fragment was used to constrain their relative position, the measured values given in the tables are measured dihedral angles.

Conclusions

A systematic study of the effect of the bridging biaryl moiety in optically active bisphosphite ligands has been described. The synthesis of eight new biaryl-based bisphosphites has been reported, along with their evaluation in rhodium-catalyzed asymmetric hydroformylation of allyl cyanide, vinyl acetate, and styrene. Comparison of the X-ray crystal structures of five square planar rhodium complexes indicates that both regio- and enantioselectivity in asymmetric hydroformylation are correlated with the dihedral angle of the bridging biaryl. DFT calculations suggest that decreased dihedral angles lead to smaller P−Rh−P bite angles of catalytic intermediates, which, ultimately, leads to improved regiocontrol. In addition, these decreased bite angles are found to lead to higher enantioselectivity in asymmetric hydroformylation.

Experimental Section

General Considerations. All syntheses and manipulations of air-sensitive materials were carried out in an inert atmosphere (nitrogen or argon) glovebox. Solvents were first saturated with nitrogen and then dried by passage through activated alumina and Q-5 catalyst prior to use. Deuterated benzene was dried over sodium/potassium alloy and filtered prior to use. NMR spectra were recorded on a Varian INOVA 300 and Mercury Vx 300 (FT 300 MHz; ^{1}H, 75 MHz; ^{13}C, 282 MHz; ^{31}P, 121 MHz) spectrometer. ^{1}H NMR data are reported as follows: chemical shift (multiplicity (br = broad, s = singlet, d = doublet, t = triplet, q = quartet, p = pentet, and m = multiplet), integration, and assignment). Chemical shifts for ^{1}H NMR data are reported in ppm downfield from internal tetramethylsilane (TMS, δ scale) using residual protons in the deuterated solvents (C_6D_6, 7.15 ppm: $CDCl_3$, 7.25 ppm) as references. ^{13}C data were determined with ^{1}H decoupling, and the chemical shifts are reported in ppm versus tetramethylsilane (C_6D_6, 128 ppm; $CDCl_3$, 77 ppm). The ^{31}P spectra were referenced to external neat H_3PO_4. Coupling constants are reported in hertz (Hz). Mass spectra (both positive and negative FAB) were recorded on a VG Autospec (S/N V190) mass spectrometer. Important peaks (relative % intensity versus base peak, assignment) are provided. Elemental analyses were performed by University of Michigan analytical services. [1,1′-Binaphthalene]-2,2′-diol, 5,5′,6,6′,7,7′,8,8′-octahydro-[1,1′-binaphthalene]-2,2′-diol, (*S*)-3,3′-di-*tert*-butyl-5,5′,6,6′-tetramethylbiphenyl-2,2′-diol, and (1,5-cyclooctadiene)Rh(acac) were purchased from Strem. All compounds were used as received. (*S*)-4,8-Di-*tert*-butyl-6-iodo-1,2,10,11-tetramethyl-5,7-dioxa-6-phospha-dibenzo[*a*,*c*]cycloheptene,[24] 4-chloro-2,6-bis(trimethylsilyl)-dinaphtho[2,1-*d*:1′,2′-*f*][1,3,2]dioxaphosphepin,[8b] and (*S*,*S*)-6,6′-((1,1′-biphenyl)-2,2′-diylbis(oxy))bis(4,8-bis(1,1-dimethylethyl)-1,2,10,11-tetramethyl-dibenzo(*d*,*f*)(1,3,2)dioxaphosphepin ((*S*,*S*)-Kelliphite)[9] were prepared by literature procedures.

Asymmetric Hydroformylation Procedure. Hydroformylation solutions were prepared by addition of ligand and $Rh(CO)_2(acac)$ stock solutions followed by addition of solvent and then olefin solution. Total volume of solution in each reactor cell was 4 mL. Ligand solutions (0.03 M in toluene) and $Rh(CO)_2(acac)$ (0.05 M in toluene) were prepared in the drybox at room temperature. The olefin mixture (styrene/allyl cyanide/vinyl acetate/dodecane 1:1:1:0.3 molar ratio) solution was prepared by mixing 11.712 g of styrene, 7.544 g of allyl cyanide, 9.681 g of vinyl acetate, and 5.747 g of dodecane. Hydroformylation reactions were conducted in an Argonaut Endeavor reactor system housed in an inert atmosphere glovebox. The reactor system consists of eight parallel, mechanically stirred pressure reactors with individual temperature and pressure controls. Upon charging the catalyst solutions, the reactors were pressurized with the desired pressure of syn gas ($CO:H_2$ 1:1) and then heated to the desired temperature while stirring at 800 rpm. The runs were stopped after 3 h by venting and cooling the system. Upon opening the reactor, 50 μL of each reaction mixture was taken out and diluted with 1.6 mL of toluene, and this solution was analyzed by gas chromatography. For analysis of styrene and vinyl acetate products, Supelco's Beta Dex 225 column was used. Temperature program: 100 °C for 5 min, then 4 °C/min to 160 °C. Retention times: 2.40 min for vinyl acetate, 6.76 (*S*) and 8.56 (*R*) min for the enantiomers of the acetic acid 1-methyl-2-oxo-ethyl ester (branched regioisomer), 11.50 min for acetic acid 3-oxo-propyl ester (linear regioisomer), 12.11 (*S*) and 12.34 (*R*) min for the enantiomers of 2-phenylpropionaldehyde (branched regioisomer), and 16.08 min for 3-phenylpropionaldehyde (linear regioisomer). For allyl cyanide product analysis, an Astec Chiraldex A-TA column was used. Temperature program: 90 °C for 7 min, then 5 °C/min to 180 °C. Retention times: 5.55 min for allyl cyanide, 14.79 (*S*) and 15.28 (*R*) min for the enantiomers of the 3-methyl-4-oxo-butyronitrile (branched regioisomer), and 19.46 for the 5-oxo-pentanenitrile (linear regioisomer).

Preparation of 6-Iodo-2,4,8,10-tetrakis(1,1-dimethylethyl)-dibenzo[*d*,*f*][1,3,2]dioxaphosphepin. To 6.72 g (14.2 mmol) of 6-chloro-2.4.8.10-tetrakis (1,1-dimethylethyl) dibenzo[*d*,*f*][1,3,2]dioxaphosphepin dissolved in 150 mL of toluene was added 3.541 g (17.7 mmol) of trimethylsilyl iodide. After stirring overnight solvent was removed under reduced pressure to give an off-white solid (7.95 g, 99.1% yield). ^{1}H NMR (C_6D_6): δ 1.25 (s, 18H, C(CH_3)$_3$), 1.51 (s, 18H, C(CH_3)$_3$), 7.29 (d, $^4J_{H-H}$ = 2.4 Hz), 7.56 (d, 2H, $^4J_{H-H}$ = 2.4 Hz). ^{13}C{^{1}H} NMR (C_6D_6): δ 31.50 (C(*C*H$_3$)$_3$), 31.91 (d, J_{C-P} = 2.7 Hz), 34.76 C(*C*H$_3$)$_3$), 35.80 (*C*(CH$_3$)$_3$), 125.36 (*C*H), 127.43 (*C*H), 133.30 (d, J_{C-P} = 4.0 Hz), 140.69 (d, J_{C-P} = 2.0 Hz), 148.08, 148.71 (d, J_{C-P} = 7.4 Hz). ^{31}P{^{1}H} NMR (C_6D_6): δ 218.79 (s).

Preparation of (1*S*)-4-Bromo-2,6-bis(trimethylsilyl)dinaphtho[2,1-*d*:1′,2′-*f*][1,3,2]dioxaphosphepin. A solution of 8.615 g (20.00 mmol) of (1*S*)-3,3′-bis(trimethylsilyl)-[1,1′-binaphthalene]-2,2′-diol and triethylamine (6.0 mL, 43 mmol) in 50 mL of toluene was added to a solution of PBr_3 (5.44 g, 20.1 mmol) in 300 mL of toluene. The solution was stirred for 18 h and then filtered. The filtrate was evaporated to an off-white solid (8.46 g, 15.7 mmol, 78.5% yield). ^{1}H NMR (C_6D_6): δ 0.47 (s, $SiMe_3$, 9H), 0.54 (47 (s, $SiMe_3$, 9H), 6.87 (m, 2H), 7.13 (t, J = 8.1 Hz, 2H), 7.26 (t, J = 8.1 Hz, 2H), 7.66 (m, 2H), 8.05 (s, 1H), 8.14 (s, 1H). ^{31}P{^{1}H} NMR (C_6D_6): δ 195.3 (s).

Preparation of (*S*,*R*,*S*)-6,6′-((1,1′-Binaphthalene)-2,2′-diylbis-(oxy))bis(4,8-bis(1,1-dimethylethyl))-1,2,10,11-tetramethyldibenzo-[*d*,*f*][1,3,2]dioxaphosphepin, (*S*,*R*,*S*)-1. To a mixture of 0.5 g (0.98 mmol) of 8-bis(1,1-dimethylethyl)-6-iodo-1,2,10,11-tetramethyldibenzo[d,f][1,3,2]dioxaphosphepim and 140.3 mg of (1*R*)-[1,1′-binaphthalene]-2,2′-diol dissolved in 4 mL of toluene was added 0.3 mL of triethylamine. A white solid appeared at once. The reaction mixture was stirred for 2 days at room temperature. The solution was filtered and the solvent was removed under reduced pressure. The white residue was dissolved in 2 mL of toluene followed by addition of 6 mL of hexane. The solution was filtered and the solvent was removed under reduced pressure. To the residue was added 4 mL of acetonitrile, and the suspension was stirred for 3 h. The white solid was collected on the frit, washed with cold acetonitrile (2 × 4 mL), and dried under reduced pressure to give 0.4148 g of product. Yield: 80.6% ^{1}H NMR (C_6D_6): δ 1.20 (s, 18H, C(CH_3)$_3$), 1.24 (s, 18H, C(CH_3)$_3$), 1.64 (s, 6H, CH_3), 1.72 (s, 6H, CH_3), 2.01 (m, 6H, CH_3), 2.09 (s, 6H, CH_3), 6.84 (ddd, 2H, $^3J_{H-H}$ = 8.3 Hz, $^3J_{H-H}$ = 6.9 Hz, $^4J_{H-H}$ = 1.2 Hz), 6.99 (s, 2H), 7.05 (ddd, 2H, $^3J_{H-H}$ = 8.1 Hz, $^3J_{H-H}$ = 6.9 Hz, $^4J_{H-H}$ = 1.2 Hz), 7.11 (s, 2H), 7.14 (d, 2H, $^3J_{H-H}$ = 8.4 Hz), 7.57 (d, 2H, $^3J_{H-H}$ = 8.1 Hz), 7.60 (d, 2H, $^3J_{H-H}$ = 9.0 Hz), 7.80 (d, 2H, $^3J_{H-H}$ = 9.0 Hz). COSY (C_6D_6): δ 6.84/(7.05, 7.14, 7.57 (weak)), 7.05/(6.84,

(24) Pastor, S. D.; Shum, S. P.; Rodebaugh, R. K.; Debellis, A. D.; Clarke, F. H. *Helv. Chim. Acta* **1993**, *76*, 900−914.

7.14, 7.75), 7.17/6.84, 7.75/(7.05, 6.84 (weak)), 7.60/7.80. NOESY (C_6D_6): δ (aliphatic region) 1.20/(6.99, 7.80), 1.24/(7.11, 7.80), 1.64/2.01, 1.72/2.09, 2.01/(1.64, 7.11), 2.09/(1.72, 6.99). $^{13}C\{^1H\}$ NMR (C_6D_6): δ 16.64 (CH_3), 16.94 (CH_3), 20.36 (CH_3), 20.56 (CH_3), 31.22 ($C(CH_3)_3$), 31.55 ($C(CH_3)_3$), 34.63 ($C(CH_3)_3$), 34.81 ($C(CH_3)_3$), 122.10 (*C*H), 123.60 (quat.), 124.85 (*C*H), 126.62 (*C*H), 127.04 (*C*H), 127.98 (*C*H), 128.05 (*C*H), 128.55 (*C*H), 129.43 (*C*H), 130.85 (quat.), 131.19 (quat.), 131.39 (quat.), 132.73 (quat.), 132.85 (t, J_{C-P} = 2.3 Hz), quat.), 134.16 (quat.), 134.80 (quat.), 135.42 (quat.), 137.75 (quat.), 138.97 (quat.), 145.38 (t, J_{C-P} = 3.8 Hz), quat.), 148.59 (quat.). HSQC (C_6D_6): δ 1.20/31.55, 1.24/31.22, 1.64/16.64, 1.72/16.94, 2.01/20.36, 2.09/20.56, 6.84/126.62, 6.99/128.55, 7.05/124.85, 7.11/128.05, 7.14/127.04, 7.57/127.98, 7.60/129.43, 7.80/122.10. $^{31}P\{^1H\}$ NMR (C_6D_6): δ 132.1. HRMS (ESI, $(M)^+$): (*m*/*z*) calcd for $C_{68}H_{76}O_6P_2Na$ 1073.502, found 1073.503. Anal. Calcd for $C_{68}H_{76}O_6P_2$: C, 77.69; H, 7.29. Found: C, 77.47; H, 7.44.

Preparation of (*S*,*S*,*S*)-6,6′-((1,1′-Binaphthalene)-2,2′-diylbis(oxy))bis(4,8-bis(1,1-dimethylethyl))-1,2,10,11-tetramethyldibenzo[*d*,*f*][1,3,2]dioxaphosphepin, (*S*,*S*,*S*)-1. A toluene solution (10 mL) of (1*S*)-[1,1′-binaphthalene]-2,2′-diol (606 mg, 2.12 mmol) and triethylamine (0.62 mL, 4.44 mmol) was added dropwise to a toluene solution (20 mL) of (11a*S*)-6-bromo-4,8-bis(1,1-dimethylethyl)-1,2,10,11-tetramethyldibenzo[*d*,*f*][1,3,2]dioxaphosphepin, (4.23 mmol). After stirring overnight, the solution was filtered and the solvent was removed from the filtrate under reduced pressure, leaving an off-white solid. To this solid was added 20 mL of acetonitrile and the resulting suspension was stirred for 20 min. A white solid was collected after filtration, washed with 5 mL of acetonitrile, and dried under reduced pressure to give 0.640 g of product. Yield: 28.8%. ^1H NMR ($CDCl_3$): δ 1.05 (s, 18H, $C(CH_3)_3$), 1.22 (s, 18H, $C(CH_3)_3$), 1.73 (s, 6H, CH_3), 1.81 (s, 6H, CH_3), 2.19 (s, 6H, CH_3), 2.28 (s, 6H, CH_3), 7.03−7.07 (m, 4H) 7.12−7.17 (m, 4H), 7.30−7.35 (m, 2H), 7.73 (d, 2H, $^3J_{H-H}$ = 8.6 Hz), 7.80 (d, 2H, $^3J_{H-H}$ = 7.8 Hz). $^{13}C\{^1H\}$ NMR ($CDCl_3$): δ 16.63 (CH_3), 16.93 (CH_3), 20.52 (CH_3), 20.60 (CH_3), 31.21 ($C(CH_3)_3$), 31.27 ($C(CH_3)_3$), 34.58 ($C(CH_3)_3$), 34.64 ($C(CH_3)_3$), 123.62 (d, J_{C-P} = 3.6 Hz), 123.93 (d, J_{C-P} = 4.3 Hz), 124.85, 126.21, 126.93 (d, J_{C-P} = 3.3 Hz), 127.66, 127.75, 128.13, 128.85, 130.47 (d, J_{C-P} = 3.1 Hz), 130.95, 131.40, 132.40 (d, J_{C-P} = 5.2 Hz), 132.57, 133.92, 134.13, 135.14, 137.71, 138.39, 144.86, 145.39 (d, J_{C-P} = 6.1 Hz), 147.53. $^{31}P\{^1H\}$ NMR ($CDCl_3$): δ 129.47. HRMS (ESI, $(M + Na)^+$): (*m*/*z*) calcd for $C_{68}H_{76}O_6P_2Na$ 1073.501, found 1073.495. Anal. Calcd for $C_{68}H_{76}O_6P_2$: C, 77.69; H, 7.29. Found: C, 77.65.; H, 7.05.

Preparation of (*S*,*R*,*S*)-6,6′-((5,5′,6,6′,7,7′,8,8′-Octahydro(1,1′-binaphthalene)-2,2′-diyl)bis(oxy))bis(4,8-bis(1,1-dimethylethyl))-1,2,10,11-tetramethyldibenzo[*d*,*f*][1,3,2]dioxaphosphepin, (*S*,*R*,*S*)-2. To a mixture of 0.7 g (1.37 mmol) of 8-bis(1,1-dimethylethyl)-6-iodo-1,2,10,11-tetramethyldibenzo[*d*,*f*][1,3,2]dioxaphosphepin and 202 mg of (1*R*)-5,5′,6,6′,7,7′,8,8′-octahydro-[1,1′-binaphthalene]-2,2′-diol dissolved in 4 mL of toluene was added 0.41 mL of triethylamine. A white solid appeared at once. The reaction mixture was stirred for 2 days at room temperature and then filtered. The solvent was removed under reduced pressure. The white residue was dissolved in 4 mL of hexane and filtered. The solution was filtered and the solvent was removed under reduced pressure. To the residue was added 4 mL of acetonitile and the suspension was stirred for 3 h. A white solid was collected on the frit, washed with cold acetonitrile (2 × 3 mL), and dried under reduced pressure to give 0.5204 g of product. Yield: 72.2%. ^1H NMR (C_6D_6): δ 1.30−1.50 (m, 8H, CH_2), 1.39 (s, 18H, $C(CH_3)_3$), 1.54 (s, 18H, $C(CH_3)_3$), 1.69 (s, 6H, CH_3), 1.80 (s, 6H, CH_3), 1.97 (m, 2H, CH_2), 2.06 (s, 6H, CH_3), 2.14 (s, 6H, CH_3), 2.51 (m, 8H, CH_2), 2.54 (m, 2H, CH_2), 6.91 (d, 2H, $^3J_{H-H}$ = 8.4 Hz), 7.08 (s, 2H), 7.20 (s, 2H), 7.51 (d, 2H, $^3J_{H-H}$ = 8.1 Hz). NOEYS1D (C_6D_6): irradiation at 6.90 ppm: NOE response at 2.54 and 7.51 ppm; irradiation at 7.08 ppm: NOE response at 1.39 and 2.14 ppm; irradiation at 7.20 ppm: NOE response at 1.54 and 2.06; irradiation at 7.51 ppm: NOE response at 1.39, 1.54, and 6.91. $^{13}C\{^1H\}$ NMR (C_6D_6): δ 16.58 (CH_3), 16.81 (CH_3), 20.36 (CH_3), 20.48 (CH_3), 22.94 (CH_2), 23.01 (CH_2), 27.56 (CH_2), 29.49 (CH_2), 31.44 (t, J_{C-P} = 2.0 Hz, $C(CH_3)_3$), 31.80 ($C(CH_3)_3$), 34.83 ($C(CH_3)_3$), 34.86 ($C(CH_3)_3$), 115.68 (p, J_{C-P} = 10.1 Hz, *C*H), 127.40 (quat.), 128.06 (2×C, *C*H), 128.72 (*C*H), 130.91 (quat.), 131.37 (quat.), 131.98 (quat.), 132.70 (quat.), 132.81 (t, J_{C-P} = 2.0 Hz), 133.90 (quat.), 135.52 (quat.), 138.24 (quat.), 138.51 (quat.), 145.59 (quat.) 145.73 (t, J_{C-P} = 4.0 Hz), quat.), 148.33 (quat.). HSQC (C_6D_6): δ 1.30−1.50/(22.94, 23.01), 1.39/31.80, 1.54/31.44, 1.69/16.58, 1.80/16.81, 1.97/27.56, 2.06/20.36, 2.14/20.48, 2.51/29.49, 2.54/27.56, 6.91/128.72, 7.08/128.06, 7.20/128.06, 7.51/115.68. $^{31}P\{^1H\}$ NMR (C_6D_6): δ 136.02. HRMS (ESI, $(M + Na)^+$): (*m*/*z*) calcd for $C_{68}H_{84}O_6P_2Na$ 1081.564, found 1081.559. Anal. Calcd for $C_{68}H_{84}O_6P_2$: C, 77.10; H, 7.99. Found: C, 76.83; H, 8.18.

Preparation of (*S*,*S*)-4,4′-((1,1′-Biphenyl)-2,2′-diylbis(oxy))bis(2,6-bis(trimethylsilyl))dinaphtho[2,1-*d*:1′,2′-*f*][1,3,2]dioxaphosphepin, (*S*,*S*)-3. A toluene solution (10 mL) of [1,1′-diphenyl]-2,2′-diol (327 mg, 1.76 mmol) and triethylamine (0.49 mL, 3.55 mmol) was added dropwise to a toluene solution (10 mL) of (1*S*)-4-bromo-2,6-bis(trimethylsilyl)dinaphtho[2,1-*d*:1′,2′-*f*]-[1,3,2]dioxaphosphepin (3.52 mmol). After stirring overnight, the solution was filtered and the solvent was removed from the filtrate under reduced pressure, leaving an off-white solid. To this solid was added 10 mL of acetonitrile, and the resulting suspension was stirred for 10 min. A white solid was collected after filtration, washed with 3 mL of acetonitrile, and dried under reduced pressure to give 0.264 g of product. Yield: 13.6%. ^1H NMR ($CDCl_3$): δ 0.15 (s, 18H, $Si(CH_3)_3$), 0.24 (s, 18H, $Si(CH_3)_3$), 5.84 (dd, 2H, $^3J_{H-H}$ = 7.4 Hz, $^4J_{H-H}$ = 1.6 Hz), 6.83−6.89 (m, 4H) 7.06−7.24 (m, 10H), 7.38 (ddd, 2H, $^3J_{H-H}$ = 7.0 Hz, $^3J_{H-H}$ = 7.8 Hz, $^4J_{H-H}$ = 1.6 Hz), 7.45 (ddd, 2H, $^3J_{H-H}$ = 7.8 Hz, $^3J_{H-H}$ = 9.6 Hz, $^4J_{H-H}$ = 0.9 Hz), 7.84 (s, 2H), 7.88 (d, 2H, $^3J_{H-H}$ = 7.9 Hz), 7.95 (d, 2H, $^3J_{H-H}$ = 7.8 Hz), 8.01 (s, 2H). $^{13}C\{^1H\}$ NMR (C_6D_6): δ −0.39 (d, J_{C-P} = 5.6 Hz, $Si(CH_3)_3$), 0.16 ($Si(CH_3)_3$), 119.79, 120.0, 122.32 (d, J_{C-P} = 5.5 Hz), 123.09, 123.83 (d, J_{C-P} = 6.8 Hz), 124.93, 125.08, 126.65, 126.91, 127.18 (d, J_{C-P} = 8.7 Hz), 127.55, 127.87, 127.99, 128.20, 128.57, 131.34, 131.54, 132.62 (d, J_{C-P} = 1.6 Hz), 133.29, 134.34 (d, J_{C-P} = 1.4 Hz), 134.65, 137.21, 137.42, 148.99, 151.57 (d, J_{C-P} = 3.9 Hz), 152.77 (d, J_{C-P} = 8.7 Hz). $^{31}P\{^1H\}$ NMR ($CDCl_3$): δ 144.89. HRMS (ESI, $(M + Na)^+$): (*m*/*z*) calcd for $C_{64}H_{64}O_6P_2Si_4Na$ 1125.315, found 1125.315. Anal. Calcd for $C_{64}H_{64}O_6P_2Si_4$: C, 69.66; H, 5.85. Found: C, 69.74; H, 5.87.

Preparation of (*S*,*R*,*S*)-4,4′-((1,1′-Binaphthalene)-2,2′-diylbis(oxy))bis(2,6-bis(trimethylsilyl))dinaphtho[2,1-*d*:1′,2′-*f*][1,3,2]dioxaphosphepin, (*S*,*R*,*S*)-4. To 800 mg (1.48 mmol) of (1*S*)-4-bromo-2,6-bis(trimethylsilyl)dinaphtho[2,1-*d*:1′,2′-*f*][1,3,2]dioxaphosphepin dissolved in 8 mL of toluene was added 212 mg (0.74 mmol) of (1*R*)-[1,1′-binaphthalene]-2,2′-diol followed by addition of 0.25 mL (1.8 mmol) of triethylamine. After stirring overnight the solution was filtered and the solvent was removed under reduced pressure, leaving an off-white solid. To this solid was added 10 mL of acetonitrile, and the solution was stirred overnight. The solid was collected on the frit, washed with 3 mL of acetonitrile, and dried under reduced pressure to give 0.576 g of product. Yield: 64.6%. The product can be crystallized from a toluene/acetonitrile solvent mixture if necessary. ^1H NMR (C_6D_6): δ 0.02 (s, 18H, $Si(CH_3)_3$), 0.10 (s, 18H, $Si(CH_3)_3$), 6.72 (ddd, 2H, $^3J_{H-H}$ = 8.4 Hz, $^3J_{H-H}$ = 5,7 Hz, $^4J_{H-H}$ = 1.2 Hz), 6.79 (ddd, 2H, $^3J_{H-H}$ = 8.7 Hz, $^3J_{H-H}$ = 5.7 Hz, $^4J_{H-H}$ = 1.2 Hz), 6.89 (tm, 2H, $^3J_{H-H}$ = 7.5 Hz), 6.93 (ddd, 2H, $^3J_{H-H}$ = 12.0 Hz, $^3J_{H-H}$ = 5.7 Hz, $^4J_{H-H}$ = 1.2 Hz), 7.06 (ddd, 2H, $^3J_{H-H}$ = 8.0 Hz, $^3J_{H-H}$ = 6.0 Hz, $^4J_{H-H}$ = 1.2 Hz), 7.14 (t, 4H, $^3J_{H-H}$ = 8.1 Hz), 7.18 (d, 4H, $^3J_{H-H}$ = 8.4 Hz), 7.30 (ddd, 2H, $^3J_{H-H}$ = 8.1 Hz, $^3J_{H-H}$ = 5.7 Hz,

$^4J_{H-H}$ = 1.2 Hz), 7.45 (d, 2H, $^3J_{H-H}$ = 8.1 Hz), 7.61 (d, 2H, $^3J_{H-H}$ = 8.1 Hz), 7.62 (d, 2H, $^3J_{H-H}$ = 9.0 Hz), 7.79 (s, 2H), 7.85 (d, 2H, $^3J_{H-H}$ = 9.0 Hz), 7.96 (s, 2H), 7.98 (d, 2H, $^3J_{H-H}$ = 8.4 Hz). $^{13}C\{^1H\}$ NMR (C_6D_6): δ 0.47 (d, J_{C-P} = 4.1 Hz, Si(CH_3)$_3$), 0.11 (Si(CH_3)$_3$), 120.93, 121.17, 121.59, 122.36, 124.14 (d, J_{C-P} = 6.0 Hz), 124.83, 125.00, 125.20, 126.58, 126.73, 126.84, 127.00, 127.48, 127.75, 128.52, 128.65, 129.69, 130.79, 130.94, 131.56, 132.57, 132.90, 134.40, 134.47, 134.68, 137.02, 137.42, 148.75 (d, J_{C-P} = 10.0 Hz), 151.21, 153.20 (d, J_{C-P} = 8.7 Hz). $^{31}P\{^1H\}$ NMR (C_6D_6): δ 141.83. HRMS (ESI, (M + Na)$^+$): (*m*/*z*) calcd for $C_{72}H_{68}O_6P_2Si_4Na$ 1225.347, found 1225.348. Anal. Calcd for $C_{72}H_{68}O_6P_2Si_4$: C, 71.85; H, 5.69. Found: C, 72.16; H, 5.43.

Preparation of (*S*,*R*,*S*)-4,4′-((5,5′,6,6′,7,7′,8,8′-Octahydro(1,1′-binaphthalene)-2,2′-diyl)bis(oxy))bis(2,6-bis(trimethylsilyl))-dinaphtho[2,1-*d*:1′,2′-*f*][1,3,2]dioxaphosphepin, (*S*,*R*,*S*)-5. A toluene solution (10 mL) of (1*R*)-5,5′,6,6′,7,7′,8,8′-octahydro-[1,1′-binaphthalene]-2,2′-diol (517 mg, 1.76 mmol) and triethylamine (0.49 mL, 3.55 mmol) was added dropwise to a toluene solution (10 mL) of (1*S*)-4-bromo-2,6-bis(trimethylsilyl)dinaphtho[2,1-*d*:1′,2′-*f*][1,3,2]dioxaphosphepin (3.52 mmol). After stirring overnight, the solution was filtered and the solvent was removed from the filtrate under reduced pressure, leaving an off-white solid. To this solid was added 10 mL of acetonitrile, and the resulting suspension was stirred for 10 min. A white solid was collected by filtration, washed with 3 mL of acetonitrile, and dried under reduced pressure to give 0.368 g of product. Yield: 17.3%. ^1H NMR ($CDCl_3$): δ 0.12 (s, 18H, Si(CH_3)$_3$), 0.36 (s, 18H, Si(CH_3)$_3$), 0.75 (m, 2H, CH_2), 0.87 (m, 2H, CH_2), 1.04 (m, 2H, CH_2), 1.13 (m, 2H, CH_2), 1.61 (ddd, 2H, $^2J_{H-H}$ = 17.0 Hz, $^3J_{H-H}$ = 7.1 Hz, $^3J_{H-H}$ = 7.1 Hz, CH_2), 1.75 (ddd, 2H, $^2J_{H-H}$ = 16.5 Hz, $^3J_{H-H}$ = 6.1 Hz, $^3J_{H-H}$ = 6.1 Hz, CH_2), 1.95 (ddd, 2H, $^2J_{H-H}$ = 17.4 Hz, $^3J_{H-H}$ = 6.1 Hz, $^3J_{H-H}$ = 6.1 Hz, CH_2), 2.26 (ddd, 2H, $^2J_{H-H}$ = 15.9 Hz, $^3J_{H-H}$ = 6.0 Hz, $^3J_{H-H}$ = 6.0 Hz, CH_2), 6.68 (d, 2H, $^3J_{H-H}$ = 8.2 Hz), 6.95 (d, 2H, $^3J_{H-H}$ = 8.5 H) 7.02 (dd, 2H, $^3J_{H-H}$ = 8.6 Hz, $^4J_{H-H}$ = 1.6 Hz), 7.07−7.18 (m, 6H), 7.34 (ddd, 2H, $^3J_{H-H}$ = 8.1 Hz, $^3J_{H-H}$ = 7.4 Hz, $^4J_{H-H}$ = 1.4 Hz), 7.40 (ddd, 2H, $^3J_{H-H}$ = 7.7 Hz, $^3J_{H-H}$ = 6.3 Hz, $^4J_{H-H}$ = 1.1 Hz), 7.79 (s, 2H), 7.86 (d, 2H, $^3J_{H-H}$ = 8.0 Hz), 7.91 (d, 2H, $^3J_{H-H}$ = 8.2 Hz), 8.01 (s, 2H). $^{13}C\{^1H\}$ NMR ($CDCl_3$): δ 0.17 (d, J_{C-P} = 3.6 Hz, Si(CH_3)$_3$), 0.56 (Si(CH_3)$_3$), 22.67 (CH_2), 22.94 (CH_2), 27.30 (CH_2), 28.81 (CH_2), 115.84, 116.01, 121.73, 123.30 (d, J_{C-P} = 5.1 Hz), 124.85, 124.92, 126.24, 126.58, 127.19, 127.30, 128.48, 128.53, 128.66, 131.02, 131.16, 132.20, 132.80, 133.03, 134.05, 134.46, 136.16, 137.08, 138.13, 147.16, 151.90, 152.08 (d, J_{C-P} = 5.6 Hz). $^{31}P\{^1H\}$ NMR ($CDCl_3$): δ 149.04. HRMS (ESI, (M + Na)$^+$): (*m*/*z*) calcd for $C_{72}H_{76}O_6P_2Si_4Na$ 1233.409, found 1233.406. Anal. Calcd for $C_{72}H_{68}O_6P_2Si_4$: C, 71.85; H, 5.69. Found: C, 71.17; H, 6.01.

Preparation of (*R*)-6,6′-((1,1′-Binaphthalene)-2,2′-diylbis-(oxy)) bis(2,4,8,10-tetrakis(1,1-dimethylethyl))dibenzo[*d*,*f*][1,3,2]-dioxaphosphepin, (*R*)-6. To a mixture of 0.80 g (1.41 mmol) of 6-iodo-2,4,8,10-tetrakis(1,1-dimethylethyl)dibenzo[*d*,*f*][1,3,2]-dioxaphosphepin and 202 mg of (1*R*)-[1,1′-binaphthalene]-2,2′-diol dissolved in 4 mL of toluene was added 0.41 mL of triethylamine. A white solid appeared at once. After stirring overnight the solution was filtered and the solvent was removed under reduced pressure. The residue was redissolved in 4 mL of hexane, then filtered. Solvent was removed under reduced pressure. To the residue was added 3 mL of acetonitrile, and the resulting suspension was stirred for 2 h. A white solid was collected on the frit, washed with 2 mL of cold acetonitrile, and dried under reduced pressure to give 0.566 g of product. Yield: 68.9%. ^1H NMR (C_6D_6): δ 1.29 (s, 72H, C(CH_3)$_3$), 6.98 (ddd, 2H, $^3J_{H-H}$ = 8.4 Hz, $^3J_{H-H}$ = 6.9 Hz, $^4J_{H-H}$ = 1.2 Hz), 7.14 (ddd, 2H, $^3J_{H-H}$ = 8.1 Hz, $^3J_{H-H}$ = 6.9 Hz, $^4J_{H-H}$ = 1.2 Hz), 7.31 (d, 2H, $^3J_{H-H}$ = 8.1 Hz), 7.37 (d, 2H, $^4J_{H-H}$ = 2.7 Hz), 7.38 (d, 2H, $^4J_{H-H}$ = 2.7 Hz), 7.51 (d, 2H, $^4J_{H-H}$ = 2.4 Hz), 7.55 (d, 2H, $^4J_{H-H}$ = 2.4 Hz), 7.58 (d, 2H, $^3J_{H-H}$ = 9.0 Hz), 7.64 (d, 2H, $^3J_{H-H}$ = 8.1 Hz), 7.65 (d, 2H, $^3J_{H-H}$ = 8.7 Hz). NOESY (C_6D_6): δ irradiation at 1.29 ppm: NOE response at 7.37 and 7.53 ppm. COSY (C_6D_6): δ 6.98/(7.14, 7.31, 7.64 (weak)), 7.14/(6.98, 7.31 (weak), 7.64), 7.31/6.98, (7.37, 7.38)/(7.51, 7.55), (7.51, 7.55)/(7.37, 7.38), 7.58 /7.65, 7.64/(6.98 (weak), 7.14), 7.65/7.58. $^{13}C\{^1H\}$ NMR (C_6D_6): δ 31.14 (C(CH_3)$_3$), 31.21 (C(CH_3)$_3$), 31.57 (C(CH_3)$_3$), 31.62 (C(CH_3)$_3$), 34.64 (C(CH_3)$_3$), 34.68 (C(CH_3)$_3$), 35.52 (C(CH_3)$_3$), 35.54 (C(CH_3)$_3$), 122.99 (d, J_{C-P} = 6.0 Hz, *C*H), 123.84 (quat.), 124.49 (*C*H), 125.07 (*C*H), 126.89 (*C*H), 127.06 (*C*H), 128.15 (*C*H), 129.39 (*C*H), 131.31 (quat.), 133.34 (quat.), 133.98 (quat.), 134.70 (quat.), 140.85 (quat.), 141.32 (quat.), 146.32 (quat.), 146.54 (quat.), 146.99 (quat.), 148.34 (quat.). HSQC (C_6D_6): δ 6.98/126.89, 7.14/125.07, 7.31/127.06, 7.37/127.06, 7.53/124.49, 7.58/122.99, 7.64/128.15, 7.65/129.39. $^{31}P\{^1H\}$ NMR (C_6D_6): δ 132.81 ($\Delta\nu_{1/2}$ = 29 Hz). HRMS (ESI, (M + Na)$^+$): (*m*/*z*) calcd for $C_{76}H_{92}O_6P_2Na$ 1185.627, found 1185.623. Anal. Calcd for $C_{76}H_{92}O_6P_2$: C, 78.45; H, 7.97. Found: C, 78.52; H, 8.40.

Preparation of (*R*)-6,6′-((5,5′,6,6′,7,7′,8,8′-Octahydro(1,1′-binaphthalene)-2,2′-diylbis(oxy))bis(2,4,8,10-tetrakis(1,1-dimethylethyl))dibenzo[*d*,*f*][1,3,2]dioxaphosphepin, (*R*)-7. To a mixture of 0.933 g (1.65 mmol) of 6-iodo-2,4,8,10-tetrakis(1,1-dimethylethyl)dibenzo[*d*,*f*][1,3,2]dioxaphosphepin and 235.8 mg of (1*R*)-5,5′,6,6′,7,7′,8,8′-octahydro-[1,1′-binaphthalene]-2,2′-diol dissolved in 4 mL of toluene was added 0.5 mL of triethylamine. A white solid appeared at once. After stirring overnight, the solution was filtered and the solvent was removed under reduced pressure. The residue was redissolved in 4 mL of hexane, then filtered. Solvent was removed under reduced pressure. To the residue was added 3 mL of acetonitrile, and the resulting suspension was stirred overnight. A white solid was collected on the frit, washed with 2 mL of cold acetonitrile, and dried under reduced pressure to give 0.7272 g of product. Yield: 68.9%. ^1H NMR (C_6D_6): δ 1.28 (s, 1H, C(CH_3)$_3$), 1.29 (s, 1H, C(CH_3)$_3$), 1.46 (br s, 8H, CH_2) 1.47 (s, 1H, C(CH_3)$_3$), 1.49 (s, 1H, C(CH_3)$_3$). 2.18 (m, 2H, CH_2), 2.57 (br s, 4H, CH_2), 2.70 (m, 2H, CH_2), 6.94 (d, 2H, $^3J_{H-H}$ = 8.1 Hz), 7.33 (d, 2H, $^4J_{H-H}$ = 2.4 Hz), 7.36 (d, 2H, $^4J_{H-H}$ = 2.4 Hz), 7.37 (d, 2H, $^3J_{H-H}$ = 8.1 Hz), 7.55 (d, 2H, $^4J_{H-H}$ = 2.4 Hz), 7.58 (d, 2H, $^4J_{H-H}$ = 2.4 Hz). NOESY1D (C_6D_6): δ 7.57/(1.28, 1.29, 1.47, 1.49), 6.94/2.57. $^{13}C\{^1H\}$ NMR (C_6D_6): δ 23.18 (CH_2), 28.08 (CH_2), 29.71 (CH_2), 31.46 (C(CH_3)$_3$), 31.59 (C(CH_3)$_3$), 34.63 (C(CH_3)$_3$), 34.66 (C(CH_3)$_3$), 35.65 (C(CH_3)$_3$), 35.68 (C(CH_3)$_3$), 119.06 (d, J_{C-P} = 11.5 Hz, *C*H), 124.23 (*C*H), 124.52 (*C*H), 127.04 (*C*H), 127.08 (*C*H), 128.86, 129.07 (*C*H), 133.20, 133.43, 134.05, 137.84, 140.81, 141.17, 146.31 (d, J_{C-P} = 5.4 Hz), 146.47, 146.75, 147.51. HSQC (C_6D_6): δ 1.28/31.59, 1.29/31.59, 1.46/23.18, 1.47/31.46, 1.49/31.46, 2.18/28.8, 2.57/29.71, 2.70/28.8, 6.94/129.07, 7.33/127.04 or 127.06, 7.36/127.04 or 127.06, 7.37/119.06, 7.55/124.23, 7.58/124.52. $^{31}P\{^1H\}$ NMR (C_6D_6): δ 137.91 ($\Delta\nu_{1/2}$ = 13.5 Hz). HRMS (ESI, (M + Na)$^+$): (*m*/*z*) calcd for $C_{76}H_{100}O_6P_2Na$ 1193.689, found 1193.683. Anal. Calcd for $C_{76}H_{100}O_6P_2$: C, 77.91; H, 8.60. Found: C, 77.57; H, 8.52.

Preparation of (*S*,*R*,*S*)-6,6′-((1,1′-Binaphthalene)-2,2′-diylbis-(oxy))bis(4,8-bis(1,1-dimethylethyl))-1,2,10,11-tetramethyldibenzo-[*d*,*f*][1,3,2]dioxaphosphepin(2,4-pentanedionato-κO,$\kappa O'$)-rhodium, [(*S*,*R*,*S*)-1]Rh(acac). To a vial containing 74 mg (0.07 mmol) of (*S*,*R*,*S*)-6,6′-((1,1′-binaphthalene)-2,2′-diylbis(oxy))bis-(4,8-bis(1,1-dimethylethyl))-1,2,10,11-tetramethyldibenzo[*d*,*f*][1,3,2]-dioxaphosphepin ((*S*,*R*,*S*)-**1**) and 22 mg (0.07 mmol) of (1,5-cyclooctadiene)Rh(acac) was added 0.7 mL of C_6D_6. The resulting solution was transferred to an NMR tube. The NMR spectrum, which was recorded 2 h after mixing, showed clean formation of the desired complex. ^1H NMR (C_6D_6): δ 0.92 (s, 18H, C(CH_3)$_3$), 1.18 (s, 6H, acac-CH_3), 1.85 (s, 6H, CH_3), 1.86 (s, 6H, CH_3), 1.88 (s, 6H, CH_3), 1.97 (s, 18H, C(CH_3)$_3$), 2.09 (s, 6H, CH_3), 2.20 (br s, 8H, COD), 5.18 (s, 1H, acac-C*H*), 5.57 (br s, 4H, COD), 6.79 (ddd, 2H, $^3J_{H-H}$ = 8.4 Hz, $^3J_{H-H}$ = 6.9 Hz, $^4J_{H-H}$ = 1.2 Hz), 6.94 (d, 2H, $^3J_{H-H}$ = 8.1 Hz), 7.00 (s, 2H), 7.06 (ddd, 2H, $^3J_{H-H}$ = 7.6 Hz, $^3J_{H-H}$ = 6.9 Hz, $^4J_{H-H}$ = 1.2 Hz), 7.27 (s, 2H), 7.51 (d, 2H,

$^3J_{H-H}$ = 8.1 Hz), 7.56 (d, 2H, $^3J_{H-H}$ = 9.3 Hz), 8.46 (d, 2H, $^3J_{H-H}$ = 9.3 Hz). COSY (C_6D_6): δ 6.79/(6.94, 7.06), 6.94/6.79, 7.06/(6.79, 7.51), 7.51/7.06, 7.56/8.46, 8.46/7.56. NOESY1D (C_6D_6): δ irradiation at 0.92 ppm: NOE response at 7.00 and 1.97; irradiation at 7.27 ppm: NOE response at 1.97 and 2.09 ppm; irradiation at 8.46 ppm: NOE response at 1.97 and 7.56 ppm. $^{13}C\{^1H\}$ NMR (C_6D_6): δ 16.86 (*C*H_3), 17.08 (*C*H_3), 20.31 (*C*H_3), 20.36 (*C*H_3), 27.30 (t, J_{C-P} = 4.7 Hz, acac-*C*H_3), 28.34 (COD), 31.74 (C(*C*H_3)$_3$), 33.75 (C(*C*H_3)$_3$), 34.84 (*C*(CH$_3$)$_3$), 35.79 (*C*(CH$_3$)$_3$), 99.88 (acac-*C*H), 121.41 (*C*H), 122.76 (quat.), 124.80 (*C*H), 126.41 (*C*H), 127.20 (*C*H), 128.00 (*C*H), 128.76 (COD), 129.16 (*C*H), 129.40 (*C*H), 129.48 (*C*H), 130.62 (quat.), 131.21 (quat.), 131.39 (quat.), 132.03 (quat.), 132.39, 134.42 (quat.), 134.75 (quat.), 135.26 (quat.), 137.89 (quat.), 138.05 (quat.), 145.21 (t, J_{C-P} = 7.3 Hz, quat.), 146.81 (quat.) 148.73 (t, J_{C-P} = 4.7 Hz, quat.), 184.27 (acac-*C*-O). HSQC (C_6D_6): δ 0.92/31.74, 1.18/27.30, 1.85/16.86, 1.86/20.31 or 20.36, 1.88/17.08, 1.97/33.75, 2.09/20.31 or 20.36, 2.20/28.34, 5.18/99.88, 5.57/128.76, 6.79/126.41, 6.94/127.19, 7.00/129.48, 7.06/124.79, 7.27/129.40, 7.51/128.00, 7.56/129.16, 8.46/121.40. $^{31}P\{^1H\}$ NMR (C_6D_6): δ 133.6 (d, $^1J_{Rh-P}$ = 314.9 Hz). HRMS (ESI, (M)$^+$): (*m*/*z*) calcd for $C_{73}H_{83}O_8P_2RhNa$ 1275.452, found 1275.448.

Preparation of (*S*,*R*,*S*)-6,6′-((5,5′,6,6′,7,7′,8,8′-octahydro(1,1′-binaphthalene)-2,2′-diyl)bis(oxy))bis(4,8-bis(1,1-dimethylethyl))-1,2,10,11-tetramethyldibenzo[*d*,*f*][1,3,2]dioxaphosphepin(2,4-pentanedionato-κ*O*,κ*O*′)rhodium, [(*S*,*R*,*S*)-2]Rh(acac). To a vial containing 75 mg (0.07 mmol) of (*S*,*R*,*S*)-6,6′-((5,5′,6,6′,7,7′,8,8′-octahydro(1,1′-binaphthalene)-2,2′-diyl)bis(oxy))bis(4,8-bis(1,1-dimethylethyl))-1,2,10,11-tetramethyldibenzo[*d*,*f*][1,3,2]-dioxaphosphepin ((*S*,*R*,*S*)-**2**) and 22 mg (0.07 mmol) of (1,5-cyclooctadiene)Rh(acac) was added 0.7 mL of C_6D_6. The resulting solution was transferred to an NMR tube. The NMR spectrum, which was recorded 4 h after mixing, showed clean formation of the desired complex. After solvent evaporation, the resulting yellow solid was also analyzed by elemental analysis. ^1H NMR (C_6D_6): δ 1.16 (s, 6H, acac-CH_3), 1.38 (s, 18H, C(CH_3)$_3$), 1.44 (m, 4H, CH_2), 1.61 (m, 4H, CH_2), 1.86 (s, 6H, CH_3), 1.89 (s, 6H, CH_3), 1.93 (s, 18H, C(CH_3)$_3$), 1.96 (s, 6H, CH_3), 2.05 (m, 4H, CH_2), 2.09 (s, 6H, CH_3), 2.20 (br s, 8H, COD), 2.53 (m, 4H, CH_2), 5.16 (s, 1H, acac-C*H*), 5.57 (br s, 4H, COD), 6.78 (d, 2H, $^3J_{H-H}$ = 8.7 Hz), 7.19 (s, 2H), 7.25 (s, 2H), 7.87 (d, 2H, $^3J_{H-H}$ = 8.7 Hz). NOEYS1D (C_6D_6): irradiation at 5.16 ppm: NOE response at 1.16 ppm; irradiation at 6.78 ppm: NOE response at 1.38 (weak), 1.93 (weak), 2.53, 7.87; irradiation at 7.87 ppm: NOE response at 1.38 (weak), 1.93, 6.78. $^{13}C\{^1H\}$ NMR (C_6D_6): δ 16.79 (*C*H_3), 16.95 (*C*H_3), 20.36 (*C*H_3), 20.42 (*C*H_3), 23.14 (*C*H_2), 23.23 (*C*H_2), 27.22 (t, J_{C-P} = 317.3 Hz), 27.73 (*C*H_2), 28.34 (COD), 29.65 (*C*H_2), 32.03 (C(*C*H_3)$_3$), 33.67 (C(*C*H_3)$_3$), 34.94 (*C*(CH$_3$)$_3$), 35.72 (*C*(CH$_3$)$_3$), 99.74 (acac-*C*H), 118.91 (*C*H), 128.32 (*C*H), 128.71 (*C*H), 128.76 (COD), 128.76 (*C*H), 129.28 (*C*H), 130.48 (quat.), 131.22 (quat.), 131.72 (quat.), 132.07 (quat.), 133.54 (quat.), 134.87 (quat.), 135.03 (quat.), 136.47 (quat.), 137. 84 (quat.), 138.20 (quat.), 146.08 (t, J_{C-P} = 7.4 Hz, *C*H, quat.), 147.00 (t, J_{C-P} = 4,0 Hz, *C*H, quat.), 147.40 (t, J_{C-P} = 4.7 Hz, *C*H, quat.), 184.21 (acac-*C*-O). HSQC (C_6D_6): δ 1.16/27.22, 1.38/32.03, 1.44/23.23, 1.61/23.14, 1.86/16.79, 1.89/16.95, 1.93/33.67, 1.96/20.42, 2.05/27.73, 2.09/20.36, 2.20/28.34, 2.53/29.65, 5.16/99.74, 5.57/128.76, 6.78/128.71, 7.19/128.32, 7.25/129.28, 7.87/118.91. $^{31}P\{^1H\}$ NMR (C_6D_6): δ 134.87 (d, $^1J_{Rh-P}$ = 315.0 Hz). HRMS (ESI, (M + Na)$^+$): (*m*/*z*) calcd for $C_{73}H_{91}O_8P_2RhNa$ 1283.514, found 1283.513. Anal. Calcd for $C_{73}H_{91}O_8P_2Rh$: C, 69.51; H, 7.27. Found: C, 69.28; H, 7.50.

Preparation of (*S*,*R*,*S*)-((4,4′-((1,1′-Binaphthalene)-2,2′-diylbis(oxy))bis(2,6-bis(trimethylsilyl))dinaphtho[2,1-*d*:1′,2′-*f*][1,3,2]-dioxaphosphepin-κ*P*4))(2,4-pentanedionato-κ*O*,κ*O*′)rhodium, [(*S*,*R*,*S*)-4]Rh(acac). To a vial containing 16.1 mg (0.05 mmol) of (1,5-cyclooctadiene)Rh(acac) was added 62.4 mg (0.05 mmol) of (*S*,*R*,*S*)-((4,4′-((1,1′-binaphthalene)-2,2′-diylbis(oxy))bis(2,6-bis-(trimethylsilyl))dinaphtho[2,1-*d*:1′,2′-*f*][1,3,2]dioxaphosphepin ((*S*,*R*,*S*)-**4**) dissolved in 0.7 mL of C_6D_6. The resulting solution was transferred to an NMR tube. The NMR spectrum, which was recorded 20 h after mixing, showed clean formation of the desired complex. ^1H NMR (C_6D_6): δ 0.00 (s, 18H, Si(CH_3)$_3$), 0.74 (s, 6H, acac-CH_3), 0.92 (s, 18H, Si(CH_3)$_3$), 2.20 (br s, 8H, COD), 4.94 (s, 1H, acac-C*H*), 5.57 (br s, 4H, COD), 6.77 (m, 4m), 6.88 (tm, 4H, $^3J_{H-H}$ = 8.4 Hz), 7.0−7.18 (m, 6H), 7.28 (d, 2H, $^3J_{H-H}$ = 8.4 Hz), 7.33 (d, 2H, $^3J_{H-H}$ = 9.3 Hz), 7.43 (t, 4H, $^3J_{H-H}$ = 7.2 Hz), 7.50 (d, 2H, $^3J_{H-H}$ = 8.1 Hz), 7.70 (d, 2H, $^3J_{H-H}$ = 7.5 Hz), 7.91 (s, 2H), 8.06 (d, 2H, $^3J_{H-H}$ = 9.3 Hz), 8.21 (s, 2H). $^{13}C\{^1H\}$ NMR (C_6D_6): δ 0.36 (Si(*C*H_3)$_3$), 2.06 (Si(*C*H_3)$_3$), 26.85 (acac-*C*H_3), 28.54 (COD), 100.09 (acac-*C*H), 121.27, 121.59, 122.44, 122.95, 124.89, 124.99, 125.05, 126.61, 126.67, 126.80, 126.92, 127.11, 127.59, 128.17, 128.51, 128.65, 128.76, 129.77, 131.30, 131.37, 131.59, 133.35, 133.48, 134.54, 134.65, 135.08, 136.95, 137.13, 148.56 (t, J_{C-P} = 5.2 Hz), 152.34 (t, J_{C-P} = 6.7 Hz), 158.81, 184.31 (acac-*C*-O). $^{31}P\{^1H\}$ NMR (C_6D_6): δ 141.5 (d, $^1J_{Rh-P}$ = 318.2 Hz). HRMS (ESI, (M + Na)$^+$): (*m*/*z*) calcd for $C_{77}H_{77}O_8P_2RhSi_4Na$ 1428.299, found 1428.297.

Preparation of (*R*)-6,6′-((1,1′-Binaphthalene)-2,2′-diylbis-(oxy))bis(2,4,8,10-tetrakis(1,1-dimethylethyl))dibenzo[*d*,*f*][1,3,2]-dioxaphosphepin(2,4-pentanedionato-κ*O*,κ*O*′)rhodium, [(*R*)-6]-Rh(acac). To a vial containing 83 mg (0.07 mmol) of (*R*)-6,6′-((1,1′-binaphthalene)-2,2′-diylbis(oxy))bis(2,4,8,10-tetrakis(1,1-dimethylethyl))dibenzo[*d*,*f*][1,3,2]dioxaphosphepin ((*R*)-**6**) and 22 mg (0.07 mmol) of (1,5-cyclooctadiene)Rh(acac) was added 0.7 mL of C_6D_6. The resulting solution was transferred to an NMR tube. The NMR spectrum, which was recorded 4 h after mixing, showed clean formation of the desired complex. ^1H NMR (C_6D_6): δ 0.98 (s, 18H, C(CH_3)$_3$), 1.15 (s, 18H, C(CH_3)$_3$), 1.18 (s, 6H, acac-CH_3), 1.31 (s, 18H, C(CH_3)$_3$), 1.95 (s, 18H, C(CH_3)$_3$), 2.20 (br s, 8H, COD), 5.20 (s, 1H, acac-C*H*), 5.57 (br s, 4H, COD), 6.76 (ddd, 2H, $^3J_{H-H}$ = 8.7 Hz, $^3J_{H-H}$ = 6.3 Hz, $^4J_{H-H}$ = 1.2 Hz), 6.81 (d, 2H, $^3J_{H-H}$ = 7.5 Hz), 7.11 (ddd, 2H, $^3J_{H-H}$ = 8.3 Hz, $^3J_{H-H}$ = 6.3 Hz, $^4J_{H-H}$ = 1.2 Hz), 7.37 (d, 2H, $^4J_{H-H}$ = 2.7 Hz), 7.42 (d, 2H, $^4J_{H-H}$ = 2.1 Hz), 7.43 (d, 2H, $^4J_{H-H}$ = 2.4 Hz), 7.58 (d, 2H, $^3J_{H-H}$ = 8.7 Hz), 7.61 (d, 2H, $^3J_{H-H}$ = 9.3 Hz), 7.64 (d, 2H, $^4J_{H-H}$ = 2.4 Hz), 8.44 (d, 2H, $^3J_{H-H}$ = 9.3 Hz). NOEYS1D (C_6D_6): irradiation at 1.95 ppm: NOE response at 0.98 (weak), 7.64 and 8.44 ppm; irradiation at 8.44 ppm: NOE response at 7.64 and 1.95 ppm. COSY (C_6D_6): δ 6.76/(6.81, 7.11, 7.58 (weak)) 6.81/6.76, 7.11/(6.76, 7.58), 7.42/7.64, 7.43/7.64, 7.58/(6.76 (weak), 7.11) 7.61/8.44, 7.64/7.43, 8.44/7.61. $^{13}C\{^1H\}$ NMR (C_6D_6): δ 27.28 (t, J_{C-P} = 4.9 Hz, acac-*C*H_3), 28.35 (COD), 31.33 (C(*C*H_3)$_3$), 31.42 (C(*C*H_3)$_3$), 31.68 (C(*C*H_3)$_3$), 33.65 (C(*C*H_3)$_3$), 34.48 (*C*(CH$_3$)$_3$), 34.59 (*C*(CH$_3$)$_3$), 35.42 (*C*(CH$_3$)$_3$), 36.48 (*C*(CH$_3$)$_3$), 99.95 (acac-*C*H), 121.59 (*C*H), 123.25 (quat.), 124.91 (*C*H), 125.25 (*C*H), 125.69 (*C*H), 126.59 (*C*H), 127.01 (*C*H), 127.59 (*C*H), 127.94 (*C*H), 128.76 (COD), 129.22 (*C*H), 131.55 (quat.), 132.46 (quat.), 133.12 (quat.), 134.48 (quat.), 140.01 (quat.), 140.62 (quat.), 145.87 (t, J_{C-P} = 8.7 Hz, quat.), 146.07 (quat.), 146.53 (quat.), 147.59 (t, J_{C-P} = 4.1 Hz, quat.), 148.18 (t, J_{C-P} = 3.9 Hz, quat.), 184.55 (acac-*C*-O). HSQC (C_6D_6): δ 0.98/31.33, 1.15/31.42, 1.18/27.28, 1.31/31.68, 1.95/33.65, 6.76/126.59, 6.81/127.01, 7.11/124.91, 7.37/125.25, 7.42/127.59, 7.43/127.59, 7.58/127.94, 7.61/129.22, 7.64/125.69, 8.44/121.58. $^{31}P\{^1H\}$ NMR (C_6D_6): δ 137.8 (d, $^1J_{Rh-P}$ = 312.8 Hz). HRMS (ESI, (M + Na)$^+$): (*m*/*z*) calcd for $C_{81}H_{99}O_8P_2$-RhNa 1387.577, found 1387.577.

Preparation of (*R*)-6,6′-((5,5′,6,6′,7,7′,8,8′-Octahydro(1,1′-binaphthalene)-2,2′-diylbis(oxy))bis(2,4,8,10-tetrakis(1,1-dimethylethyl))dibenzo[*d*,*f*][1,3,2]dioxaphosphepin(2,4-pentanedionato-κ*O*,κ*O*′)rhodium, [(*R*)-7]Rh(acac). To a vial containing 91 mg (0.08 mmol) of (*R*)-6,6′-((5,5′,6,6′,7,7′,8,8′-octahydro(1,1′-binaphthalene)-2,2′-diylbis(oxy))bis(2,4,8,10-tetrakis(1,1-dimethylethyl))dibenzo[*d*,*f*][1,3,2]dioxaphosphepin ((*R*)-**7**) and 25.3 mg (0.08 mmol) of (1,5-cyclooctadiene)Rh(acac) was added 0.7

mL of C_6D_6. The resulting solution was transferred to an NMR tube. The NMR spectrum, which was recorded 5 h after mixing, showed formation of the desired complex. ^{1}H NMR (C_6D_6): δ 1.19 (s, 3H), 1.22 (s, 1H, C(CH_3)$_3$), 1.29 (s, 1H, C(CH_3)$_3$), 1.41 (m, 4H, CH_2), 1.42 (s, 1H, C(CH_3)$_3$), 1.62 (m, 4H, CH_2), 1.91 (s, 1H, C(CH_3)$_3$), 2.05 (m, 4H, CH_2), 2.6 (m, 4H, CH_2), 5.19 (s, 1H, C*H*-acac), 6.83 (d, 2H, $^3J_{H-H}$ = 8.7 Hz), 7.40 (d, 2H, $^4J_{H-H}$ = 2.4 Hz) 7.45 (d, 2H, $^4J_{H-H}$ = 2.4 Hz), 7.57 (d, 2H, $^4J_{H-H}$ = 2.4 Hz), 7.62 (d, 2H, $^4J_{H-H}$ = 2.4 Hz), 7.88 (d, 2H, $^3J_{H-H}$ = 8.7 Hz). NOESY1D (C_6D_6): δ irradiation at 7.88 ppm: NOE response at 6.83 and 1.91 ppm; irradiation at 6.83 ppm: NOE response at 7.88 and 2.59 ppm. ^{13}C{^{1}H} NMR (C_6D_6): δ 23.12 (*C*H$_2$), 23.34 (*C*H$_2$), 27.22 (acac-*C*H$_3$), 27.48 (*C*H$_2$), 29.75 (*C*H$_2$), 31.53 (C(*C*H$_3$)$_3$), 31.66 (C(*C*H$_3$)$_3$), 31.71 (C(*C*H$_3$)$_3$), 33.57 (C(*C*H$_3$)$_3$), 34.55 (*C*(CH$_3$)$_3$), 34.59 (*C*(CH$_3$)$_3$), 35.59 (*C*(CH$_3$)$_3$), 36.46 (*C*(CH$_3$)$_3$), 100.0, 119.14 (C*H*), 124.31 (C*H*), 125.56 (C*H*), 127.68 (C*H*), 128.80 (C*H*), 132.22, 133.11, 133.75, 136.71, 140.03, 140.71, 145.79, 146.42, 146.68 (d, J_{C-P} = 8.9 Hz), 146.98, 147.75 (t, J_{C-P} = 4.1 Hz), 184.51 (acac-*C*-O). HSQC (C_6D_6): δ 1.19/27.22, 1.22/31.53, 1.29/31.66, 1.41/23.12 or 23.34, 1.42/31.71, 1.62 23.12 or 23.34, 1.91/33.57, 2.05/27.48, 2.60/29.75, 5.19/100.0, 6.83/128.80, 7.40/127.68, 7.45/127.68, 7.57/124.31, 7.62/125.56, 7.88/119.14. ^{31}P{^{1}H} NMR (C_6D_6): δ 138.35 (d, $^1J_{Rh-P}$ = 312.8 Hz). HRMS (ESI, (M + Na)$^+$): (*m*/*z*) calcd for $C_{81}H_{107}NaO_8P_2Rh$ 1395.639, found 1395.634.

X-ray Analysis of (*S*,*S*)-3, Rh-Dimer, [(*S*,*R*,*S*)-1]Rh(acac), [(*S*,*R*,*S*)-2]Rh(acac), [(*S*,*R*,*S*)-4]Rh(acac), and [(*R*)-7]Rh(acac). Data for all structures were collected at 173 K on a Siemens SMART PLATFORM equipped with a CCD area detector and a graphite monochromator utilizing Mo Kα radiation (λ = 0.71073 Å). Cell parameters were refined using up to 8192 reflections. A hemisphere of data (1381 frames) was collected using the ω-scan method (0.3° frame width) for each structure. The first 50 frames were remeasured at the end of data collection to monitor instrument and crystal stability (maximum correction on *I* was <1%). Absorption corrections by integration were applied on the basis of measured indexed crystal faces. The structures were solved by the direct methods in SHELXTL6[25] and refined using full-matrix least-squares. The non-H atoms were treated anisotropically, whereas the methyl hydrogen atoms were calculated in ideal positions and were riding on their respective carbon atoms. For (*S*,*S*)-**3**, a total of 781 parameters were refined in the final cycle of refinement using 9503 reflections with $I > 2\sigma(I)$ to yield R_1 and wR_2 of 4.41% and 8.91%, respectively. For **Rh-dimer**, a total of 492 parameters were refined in the final cycle of refinement using 7056 reflections with $I > 2\sigma(I)$ to yield R_1 and wR_2 of 4.41% and 9.97%, respectively. For [(*S*,*R*,*S*)-**1**]Rh(acac), a total of 758 parameters were refined in the final cycle of refinement using 10 590 reflections with $I > 2\sigma(I)$ to yield R_1 and wR_2 of 3.28% and 6.30%, respectively. For [(*S*,*R*,*S*)-**2**]Rh(acac), a total of 751 parameters were refined in the final cycle of refinement using 11 592 reflections with I > 2σ(*I*) to yield R_1 and wR_2 of 3.78% and 9.08%, respectively. In addition to the complex, the asymmetric unit contains two acetone molecules of crystallization. The latter were disordered and could not be modeled properly; thus the program SQUEEZE,[26] a part of the PLATON[27] package of crystallographic software, was used to calculate the solvent disorder area and remove its contribution to the overall intensity data. For [(*S*,*R*,*S*)-**4**]Rh(acac), a total of 829 parameters were refined in the final cycle of refinement using 8280 reflections with $I > 2\sigma(I)$ to yield R_1 and wR_2 of 5.40% and 8.43%, respectively. For [(*R*)-**7**]Rh(acac), a total of 1645 parameters were refined in the final cycle of refinement using 29 638 reflections with $I > 2\sigma(I)$ to yield R_1 and wR_2 of 5.31% and 12.71%, respectively. The asymmetric unit contains two crystallographically independent but chemically equivalent complexes. Five hexane molecules were located in the asymmetric unit. They were disordered and could not be modeled properly; thus the program SQUEEZE was used to calculate the solvent disorder area and remove its contribution to the overall intensity data. The complexes have a total of seven disordered moieties. Each one was refined in two parts with their site occupation factors dependently refined. All atoms of the disordered moieties were refined with isotropic thermal parameters. Refinement was done using F^2.

Structure of (*S*,*S*)-**3**: $C_{70}H_{73}N_3O_6P_2Si_4$, MW = 1226.61, orthorhombic, $P2_12_12_1$, colorless needle (0.31 × 0.20 × 0.15 mm^3), a = 9.6032(6) Å, b = 21.6943(13) Å, c = 32.986(2) Å, temp = 173(2) K, Z = 4, V = 2592 Å^3, R1 = 0.0441, 0.0878, wR2 = 0.0891, 0.0985 ($I > 2\sigma(I)$, all data), GOF = 0.916.

Structure of **Rh-dimer**: $C_{84}H_{116}O_6P_2Rh_2$, MW = 1489.53, triclinic, $P\bar{1}$, yellow plate (0.18 × 0.13 × 0.04 mm^3), a = 11.1580(6) Å, b = 12.8010(7) Å, c = 14.2385(8) Å, α = 91.730(1)°, β = 104.682(1)°, γ = 100.154(1)°, temp = 173(2) K, Z = 1, V = 1930.52(18) Å^3, R1 = 0.0441, 0.0600, wR2 = 0.0997, 0.1067 ($I > 2\sigma(I)$, all data), GOF = 1.019.

Structure of [(*S*,*R*,*S*)-**1**]Rh(acac): $C_{73}H_{83}O_8P_2Rh$, MW = 1253.24, orthorhombic, $P2_12_12_1$, yellow needle (0.31 × 0.20 × 0.15 mm^3), a = 13.2638(7) Å, b = 21.4089(11) Å, c = 23.2485(12) Å, temp = 173(2) K, Z = 4, V = 6601.7(6) Å^3, R1 = 0.0328, 0.0501, wR2 = 0.0630, 0.0647 ($I > 2\sigma(I)$, all data), GOF = 0.858.

Structure of [(*S*,*R*,*S*)-**2**]Rh(acac): $C_{79}H_{103}O_{10}P_2Rh$, MW = 1377.46, orthorhombic, $P2_12_12$, yellow plate (0.19 × 0.15 × 0.06 mm^3), a = 17.472(1) Å, b = 25.208(2) Å, c = 16.684(1) Å, temp = 173(2) K, Z = 4, V = 7348.1(7) Å^3, R1 = 0.0418, 0.0662, wR2 = 0.0913, 0.0960 ($I > 2\sigma(I)$, all data), GOF = 0.899.

Structure of [(*S*,*R*,*S*)-**4**]Rh(acac): $C_{77}H_{75}O_8P_2RhSi_4$, MW = 1405.58, orthorhombic, $P2_12_12_1$, yellow prism (0.11 × 0.07 × 0.06 mm^3), a = 13.7261(9) Å, b = 21.6693(15) Å, c = 23.9170(15) Å, temp = 173(2) K, Z = 4, V = 7113.8(8) Å^3, R1 = 0.0540, 0.1007, wR2 = 0.0843, 0.0964 ($I > 2\sigma(I)$, all data), GOF = 0.913.

Structure of [(*R*)-**7**]Rh(acac): $C_{192}H_{284}O_{16}P_4Rh_2$, MW = 3177.89, monoclinic, $P2_1$, dark yellow plate (0.32 × 0.28 × 0.19 mm^3), a = 12.2659(9) Å, b = 28.620(2) Å, c = 26.4585(19) Å, β = 100.816(1)°, temp = 173(2) K, Z = 2, V = 9123.3(12) Å^3, R1 = 0.0531, 0.0708, wR2 = 0.1271, 0.1336 ($I > 2\sigma(I)$, all data), GOF = 0.987.

Computational Study. All calculations were performed with the Gaussian98[28] program. Optimizations were carried out using the hybrid density functional theory (DFT) method, B3LYP,[29] and a basis set of LANL2DZ[30] on rhodium and 6-31G*(5d)[31] on all other atoms.

(25) Sheldrick, G. M. *SHELXTL6*; Bruker-AXS: Madison, WI, 2002.
(26) van der Sluis, P.; Spek, A. L. *Acta Crystallogr.* **1990**, *A46*, 194−201.
(27) Spek, A. L. *Acta Crystallogr.* **1990**, *A46*, C-34.
(28) Frisch, M. J.; Trucks, G. W.; Schlegel, H. B.; Scuseria, G. E.; Robb, M. A.; Cheeseman, J. R.; Zakrzewski, V. G.; Montgomery, J. A., Jr.; Stratmann, R. E.; Burant, J. C.; Dapprich, S.; Millam, J. M.; Daniels, A. D.; Kudin, K. N.; Strain, M. C.; Farkas, O.; Tomasi, J.; Barone, V.; Cossi, M.; Cammi, R.; Mennucci, B.; Pomelli, C.; Adamo, C.; Clifford, S.; Ochterski, J.; Petersson, G. A.; Ayala, P. Y.; Cui, Q.; Morokuma, K.; Salvador, P.; Dannenberg, J. J.; Malick, D. K.; Rabuck, A. D.; Raghavachari, K.; Foresman, J. B.; Cioslowski, J.; Ortiz, J. V.; Baboul, A. G.; Stefanov, B. B.; Liu, G.; Liashenko, A.; Piskorz, P.; Komaromi, I.; Gomperts, R.; Martin, R. L.; Fox, D. J.; Keith, T.; Al-Laham, M. A.; Peng, C. Y.; Nanayakkara, A.; Challacombe, M.; Gill, P. M. W.; Johnson, B.; Chen, W.; Wong, M. W.; Andres, J. L.; Gonzalez, C.; Head-Gordon, M.; Replogle, E. S.; Pople, J. A. *Gaussian98*, Revision A.10; Gaussian, Inc.: Pittsburgh, PA, 2001.
(29) (a) Becke, A. D. *J. Chem. Phys.* **1993**, *98*, 5648−5652. (b) Lee, C.; Yang, W.; Parr, R. G. *Phys. Rev B* **1988**, *37*, 785−789. (c) Miehlich, B.; Savin, A.; Stoll, H.; Preuss, H. *Chem. Phys. Lett.* **1989**, *157*, 200−206.
(30) (a) Dunning, T. H., Jr.; Hay, P. J. In *Modern Theoretical Chemistry*; Schaefer, H. F., III, Ed.; Plenum: New York, 1977; Vol. 3, pp 1−27. (b) Hay, P. J. Wadt, W. R. *J. Chem. Phys.* **1985**, *82*, 270−283. (c) Wadt, W. R; Hay, P. J. *J. Chem. Phys.* **1985**, *82*, 284−298. (d) Hay, P. J. Wadt, W. R. *J. Chem. Phys.* **1985**, *82*, 299−310.
(31) (a) Ditchfield, R.; Hehre, W. J.; Pople, J. A. *J. Chem. Phys.* **1971**, *54*, 724−728. (b) Hehre, W. J.; Ditchfield, R.; Pople, J. A. *J. Chem. Phys.* **1972**, *56*, 2257−2261. (c) Gordon, M.S. *Chem. Phys. Lett.* **1980**, *76*, 163−168.

Acknowledgment. The authors thank Dowpharma for financial support of this work.

Supporting Information Available: Thermal ellipsoid drawings (with full labeling scheme), stereoview drawings, and comprehensive crystallographic data including CIF files of (*S*,*S*)-**3**, **Rh-dimer**, [(*S*,*R*,*S*)-**1**]Rh(acac), [(*S*,*R*,*S*)-**2**]Rh(acac), [(*S*,*R*,*S*)-**4**]Rh(acac), and [(*R*)-**7**]Rh(acac). This material is available free of charge via the Internet at http://pubs.acs.org.

OM061065Z